DESIGN, CONSTRUCTION AND PERFORMANCE MONITORING OF COVER SYSTEMS FOR WASTE ROCK AND TAILINGS

VOLUME 2 – THEORY AND BACKGROUND

MEND 2.21.4b

This work was done on behalf of MEND and sponsored by:
MEND and INCO Ltd.

July 2004

Natural Resources Canada CANMET | Ressources naturelles Canada CANMET

DESIGN, CONSTRUCTION AND PERFORMANCE MONITORING OF COVER SYSTEMS FOR WASTE ROCK AND TAILINGS

MEND 2.21.4

VOLUME 2

THEORY AND BACKGROUND

Prepared for MEND

Funded by INCO Ltd.

Edited by:

O'Kane Consultants Inc.
Integrated Geotechnical Engineering Services
Specialists in Unsaturated Zone Hydrology

OKC Report No. 702-01

July 2004

SUMMARY

This manual includes a summary volume (Volume 1) and the following four supporting technical documents:

- Volume 2 – Theory and Background;
- Volume 3 – Site Characterization and Numerical Analyses of Cover Performance;
- Volume 4 – Field Performance Monitoring and Sustainable Performance of Cover Systems; and
- Volume 5 – Case Studies.

The basic theory discussed in Volume 2 focuses on unsaturated zone hydrology as it relates to the design of cover systems. Volume 2 is divided into two sections. Section 1 presents the background theory and fundamental concepts pertinent to soil cover design. The topics are grouped into four key areas: moisture storage, moisture flow, evaporation and transpiration, and oxygen transport. Moisture storage includes discussion of the topics of volume / mass relationships, the definition of soil suction, and an introduction to the relationship between soil suction and water content, referred to as the soil water characteristic curve. Moisture flow is divided into liquid flow, and includes a description of the hydraulic conductivity function and vapour flow, as well as a discussion on vapour diffusion. Lastly, evaporation, transpiration, and oxygen transport, specifically oxygen diffusion, are discussed.

Section 2 of this volume introduces applications of the basic theory to issues encountered with soil cover design. Examples illustrating the basic theory and concepts are provided. This section is divided into four subjects: moisture flow issues, moisture storage, capillary barriers, and oxygen transport. Flow issues discussed include bypass flow, basal inflow, wetting, and pore-water velocity. For the discussion of storage, an example is given for calculation of the storage capacity of a soil cover. Capillary barriers are also discussed, along with issues of capillary barriers on sloping surfaces and an example of a diversion length calculation. Lastly, the mechanisms of oxygen ingress are discussed.

TABLE OF CONTENTS

LIST OF TABLES

LIST OF FIGURES

1 BASIC THEORY AND FUNDAMENTAL CONCEPTS

The principle phenomenon of interest in soil cover design is the transient flow of water within unsaturated soil. Two fundamental processes describe any transient phenomenon: flow and storage. In the case of the soil cover, the primary issues of concern are the mechanisms responsible for the storage and movement of water in unsaturated soil.

The basic theory discussed in this volume focuses on unsaturated zone hydrology. Fundamental relationships and concepts relating to moisture storage and flow, evaporation, transpiration, and oxygen transport are presented and discussed. Some of this information was presented in the summary volume (Volume 1) but is re-stated here for clarity. Section 2 of this volume introduces applications of the basic theory to issues encountered with soil cover design such as bypass flow, cover storage, capillary barriers, and oxygen ingress mechanisms.

1.1 Storage

1.1.1 Volume/Mass Relationships

An unsaturated soil is comprised of three principal phases: solid soil particles, water, and air. A set of simple terminology is required to define the mass and volume relationships for these phases. Figure 1.1 shows a schematic representation of an elemental soil volume. The darker solid material, (S), can be viewed as the soil grains, whereas the voids are filled with water, (W) or air (A). Therefore, the total volume, V_t, is the sum of the volume of solids, V_s, and the volume of voids, V_v.

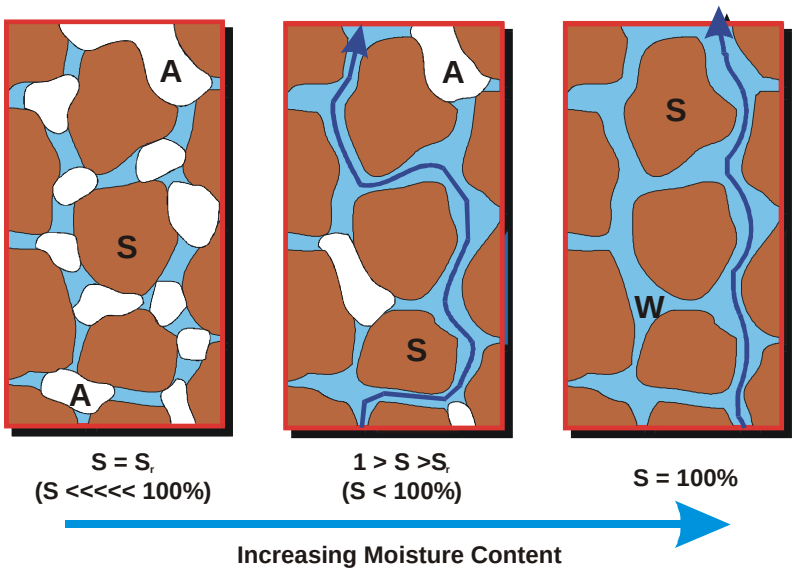

Figure 1.1 Schematic representation of a soil mass consisting of solids (S) with voids in between filled with water (W) and air (A) (CANMET, 2002).

In geotechnical practice, the volume of the voids (V_v) is often defined relative to the volume of the solids (V_s) using the term "void ratio" and the symbol "e" (i.e. $e = V_v/V_s$). If the volume of soil is taken to be equal to unity, then the volume of voids is equal to "*e*" and the total volume is then equal to (1+*e*). The volume of solids can be calculated from the mass of solids divided by the density of the solid particles. The porosity of a soil (*n*) is defined as the volume of voids divided by the total volume (V_v/V_t). This can be related to the void ratio (*e*) using the relationship *e*/(1+*e*).

Geotechnical engineers also routinely measure gravimetric water content (ω) given by the mass of water relative to the mass of dry solids. However, in dealing with the volume of water stored within a soil, it is preferable to work with volumetric water content (θ) defined as the volume of water divided by the volume total (V_w/V_t). The relationship between gravimetric water content and volumetric water content is given by the following equation:

$$\frac{\omega \rho_d}{\rho_w} = \theta \qquad [1.1]$$

where ρ_d is the dry bulk density (i.e. mass of solid / volume total) and ρ_w is the density of water.

The degree of saturation (*S*) is defined as:

$$S = {V_w}/{V_v} \times 100\% \qquad [1.2]$$

and is a calculated percentage of the volume of voids that contain water. It can also be calculated from the following equation:

$$Se = \omega G_s \qquad [1.3]$$

where G_σ is the specific gravity (i.e. ratio of the density of soil particles to the density of water).

The degree of saturation is related to the volumetric water content and the porosity through the relationship:

$$\theta = Sn \qquad [1.4]$$

If the soil is completely dry (i.e. the volume of water equals zero) then the degree of saturation is zero, while if the pores are filled with water then the degree of saturation is 100% and the volumetric water content is equal to the porosity.

In reality, a small amount of water will always be present in the voids, as represented schematically in the left most portion of Figure 1.1 where *S* <<<< *100%*.

A central concept in the performance of soil covers is the ability to relate the change in the volume of water stored in the cover to a net flux into the cover. Consider the simple cover shown in Figure 1.2. The initial volumetric water content (θ) within the cover is approximately 10% and the cover is one metre thick (Figure 1.2a). Because the definition of volumetric water content is the volume of water divided by the volume total, we can multiply the thickness of the cover (1 m) by the initial volumetric water content (10%) to calculate that the volume of water stored in the cover is 0.1 m^3 for every square metres of cover surface area. If an additional 150 mm of water was added to this cover, then the water content would have to increase from 10% to 25% (Figure 1.2b). The maximum amount of water that could be stored in this soil at saturation can be calculated from the saturated volumetric water content, equal to the porosity. If the porosity of this soil was 30%, then the maximum volume of water within the cover (at saturation) would be 300 mm.

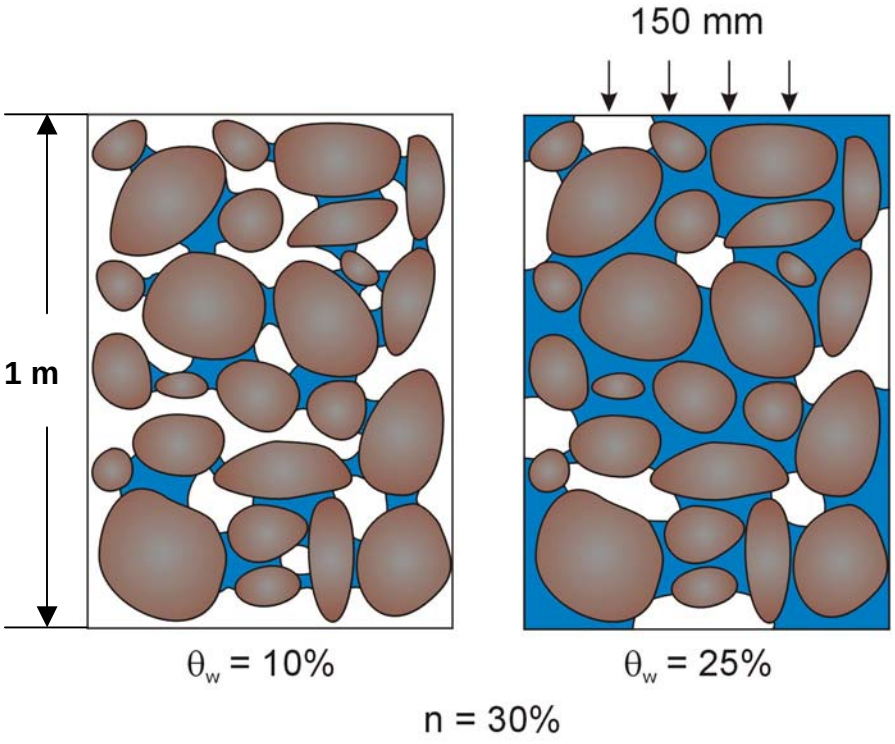

Figure 1.2 Schematic representation of a soil cover illustrating the change in water distribution in soil based on pore size.

1.1.2 Definition of Suction

Soil is generally hydrophilic; that is, soil tends to adsorb and hold moisture on its surface. When you try to remove water from a saturated soil by draining, small interfaces or menisci form between the air moving into the pores of the soil and the water, much like the menisci in capillary tubes. The air pressure can be assumed to be at atmospheric or "zero gauge" pressure relative to atmospheric pressure. The concave shape of the meniscus shows that the water pressure is less than the

atmospheric pressure. The matric suction within the soil is defined as this differential pressure between the air pressure and the water pressure in the soil. If the air pressure is assumed to be negative, then "suction", is a positive value for a negative water pressure. For example, if the soil has a suction of 100 kPa, it is under a negative water pressure of 100 kPa.

The negative pore-water pressure condition is the result of capillary and adsorptive forces that attract and bind water in the soil matrix, consequently matric suction has also been referred to in the literature as the "capillary potential". The conceptual model for matric suction is that of a capillary tube where the soil pores form the tube and the meniscus is formed by surface tension within the soil pore. This is illustrated in Figure 1.3, where water raised in a capillary tube, like water in an unsaturated soil matrix, possesses a negative pressure potential.

Figure 1.3 illustrates that under hydrostatic conditions (no flow) the total mechanical energy (total head, h) in the water above the water table (water pressure equal to zero) is the same as that below the water table even though the pressure head (h_ψ) and elevation head (h_z) vary. The negative water pressure within the soil simply represents a level of mechanical energy present in the water as a result of pore-water pressure.

It is important to note that the energy within the water may also vary as a result of changes in pore-water chemistry. If this energy is referenced to a "pure water at zero water pressure" then suction should be defined as "total suction" comprised of both matric and osmotic components (Fredlund and Rahardjo, 1993).

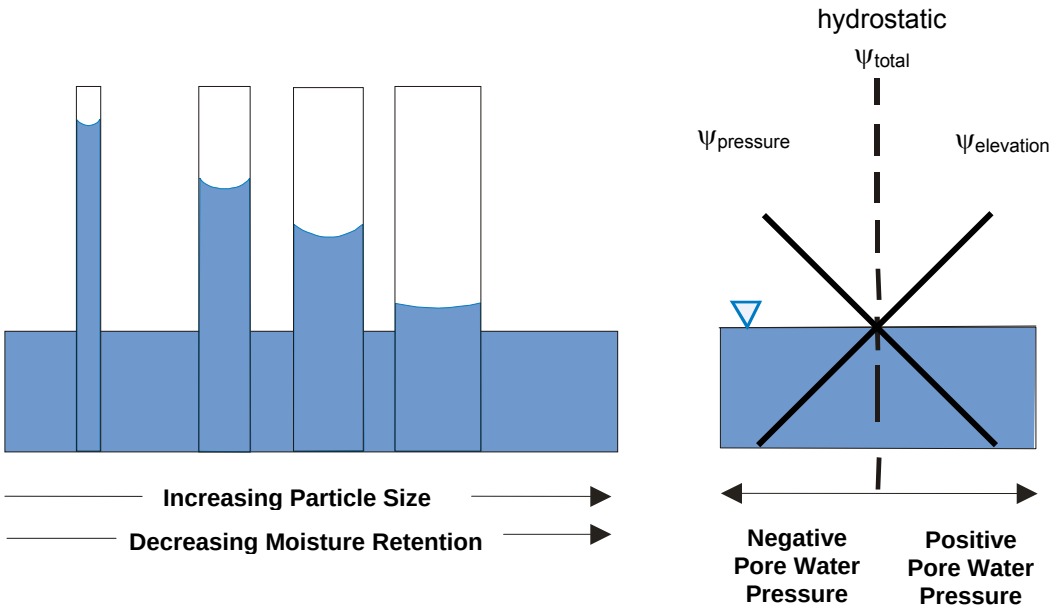

Figure 1.3 Sub-atmospheric pressure within a capillary tube (after Fredlund and Rahardjo, 1993).

1.1.3 Soil Water Characteristic Curve

The simple example provided in Figure 1.3 illustrates that pores of different sizes will tend to drain at varying levels of suction. In a soil, the pores are not a single size but are variable depending on the particle size and structure of the soil. If a soil is initially saturated and the suction within the soil is gradually increased, the largest pores would be the first to drain followed by smaller and smaller pores as the suction continues to increase. This results in changes in the volumetric water content of the sample with changes in suction. This relationship is referred to as the Soil Water Characteristic Curve (SWCC) or moisture retention curve.

Measurement of the SWCC is central to the design of any unsaturated system, such as a cover system, because it describes the fundamental relationship between the energy state of the pore-water and the volume of water stored within the soil pores. Figure 1.4 presents typical SWCCs for fine and coarse-textured materials. The negative pore-water pressure required to initiate drainage of an initially saturated soil is called the air entry value (AEV). The SWCC can be obtained from a laboratory test in which the volumetric water content of a soil sample is measured at different applied suctions or from an interpretation of field monitoring of suction and water content.

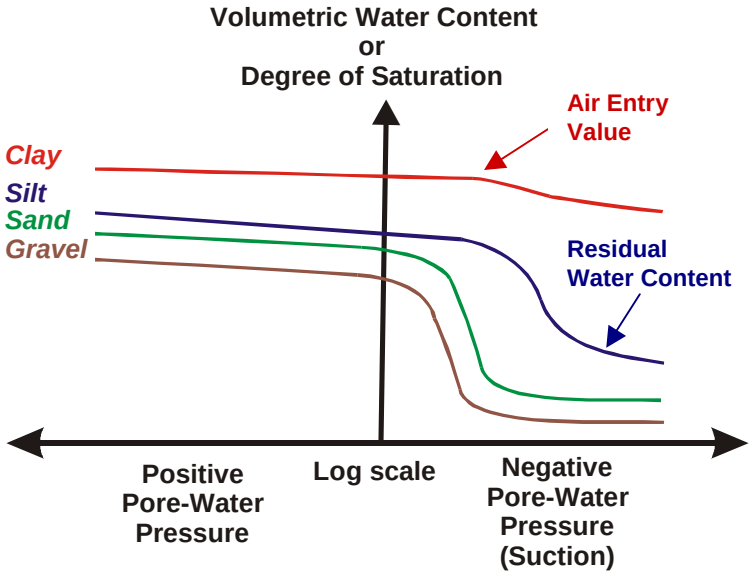

Figure 1.4 The soil water characteristic curve for different soil types (after Freeze and Cherry, 1979).

A finer textured material has the ability to retain moisture under higher suction values as compared to the coarse material because of smaller pore sizes. Hence, the coarser textured material starts to "drain" first as suction is increased from saturated conditions, and de-saturates as suction continues to increase. In contrast, the finer textured material remains at the saturated volumetric water content for the same suction condition. This phenomenon is referred to as "tension saturated" conditions.

Ultimately, the finer textured material will also begin to drain as the suction is increased. The rate at which the water content decreases with increasing suction is a function primarily of the particle size distribution and soil structure of the material. The latter factor in fine-textured soils is strongly influenced by factors such as compaction conditions, as well as the effects of freeze-thaw or wet-dry cycles. A uniform material will tend to drain "rapidly" over a small range of suction values because the pore sizes are generally the same size. Well-graded materials will have a moderate slope to the SWCC once drainage conditions are initiated because they possess a wide range of pore sizes.

As suction increases past the AEV, the soil continues to drain until the residual water content is reached. The residual water content is characterized by the relatively flat portion of the SWCC at high suctions where large increases in suction result in very small changes in water content. At water contents greater than the residual water content, water movement in soils is primarily through liquid water flow. At water contents less than the residual water content, water movement is dominated by vapour flow because the remaining water is bound more tightly to the soil particles.

Soil structure, aggregation, void ratio, type of soil, soil texture, mineralogy, stress history, and weathering effects are all factors that influence the behaviour of the SWCC (Vanapalli, 1994). Stress history and initial moulding water content probably have the most influence on soil structure and aggregation and therefore indirectly impact the nature of the SWCC, especially for a compacted soil. Specimens of a particular soil, despite having the same texture and mineralogy, can exhibit different soil water characteristic curves if they are prepared at different initial moulding water contents and possess different stress histories. The engineering behaviour of each of the specimens will differ as a result. The key factors affecting the shape of a SWCC are discussed below.

Hysteresis in the relationship between volumetric water content and suction has been observed (Freeze and Cherry, 1979); the SWCC has a different shape, depending on whether the soil is drying or wetting. Figure 1.5 is a schematic illustration of the effect of hysteresis on the SWCC. Figure 1.5 demonstrates that if the soil was initially saturated at a positive pressure head and then suction was increased to a high level, the corresponding moisture contents would follow the drying or drainage curve. The pressure heads would return along the wetting or imbibition curve if the suction was decreased and water was made available to the soil. The internal lines are scanning curves and show the path that the volumetric water content suction relationship would follow if the soil did not reach its full hysteretic loop.

Many factors cause hysteresis in soils, however the primary cause is the non-uniform pore size distribution present in a soil (Fredlund and Rahardjo, 1993). The non-uniform pore size distribution prevents the full development of capillary rise in the soil. The presence of entrapped air in the soil will also reduce the water content of the soil as the suction decreases.

Hysteresis in the SWCC of a non-uniform soil occurs at low suctions due to the capillary effect of liquid water. The effect of hysteresis at high suctions is small since vapour movement is predominant. Recent research on hysteresis can be found in Pham *et al.* (2002, 2003a and 2003b) and Fredlund *et al*. (2003)

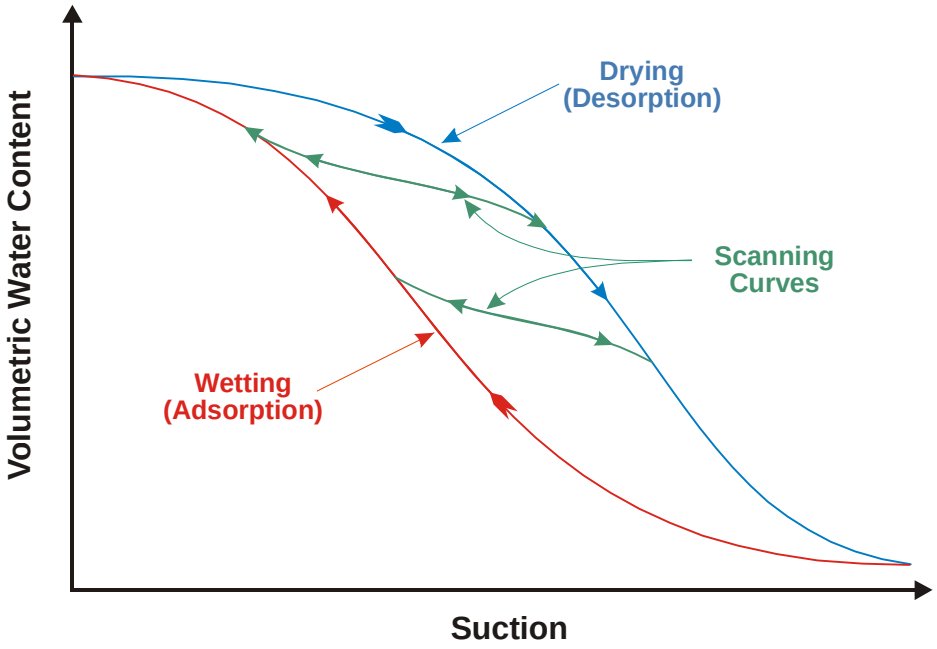

Figure 1.5 Effect of hysteresis on the soil water characteristics curve (after Liakopoulos, 1965).

1.2 Flow

The two dominant processes producing water movement in unsaturated soil are the flow of liquid water, primarily under hydraulic gradients, and the movement of water vapour as a result of vapour pressure gradients. At low suctions (high water content), liquid water flow dominates, whereas at high suctions (those greater than that corresponding to the residual water content) moisture flow occurs due to vapour flow.

1.2.1 Liquid Flow – The Hydraulic Conductivity Function

Hydraulic conductivity is the soil property that characterizes the ability of the soil to transmit fluid. Water will move through soil in response to energy gradients. These gradients are commonly due to mechanical energy gradients (e.g. total head comprised of pressure head and elevation head) but may also be due to thermal, electrical, or chemical energy gradients (Mitchell, 1976).

Liquid water flow occurs in response to a mechanical energy gradient and the relationship between a unit flux of water and the energy gradient is commonly referred to as Darcy's Law:

$$q = -ki \qquad [1.5]$$

where q = unit flux of water ($m^3/s/m^2$), k = hydraulic conductivity (m/s) and i = energy gradient (unitless).

Darcy's Law is applicable to soil, regardless of whether it is saturated or unsaturated. The key difference, however, is that the hydraulic conductivity of a saturated soil is often taken as a constant whereas the hydraulic conductivity of an unsaturated soil will change with the degree of saturation or volumetric water content (See Figure 1.6). Because the volumetric water content can be related to suction through the SWCC then this function can also be described by a relationship between hydraulic conductivity and suction as shown in Figure 1.7. Detailed descriptions of the theory of water flow in unsaturated soils are well defined by Freeze and Cherry (1979), Fredlund and Rahardjo (1993), and Guymon (1994).

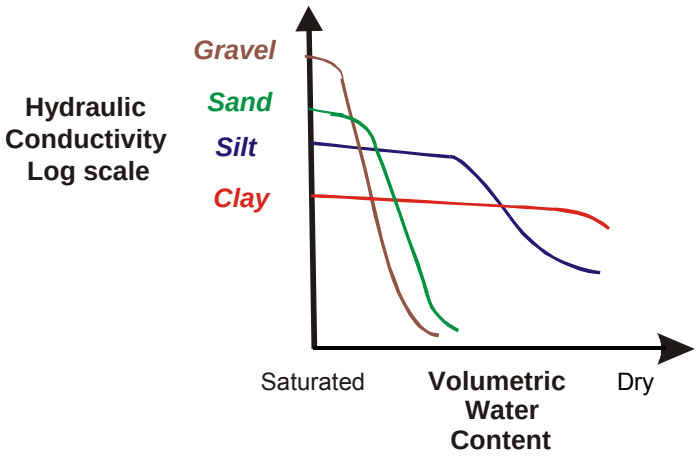

Figure 1.6 The hydraulic conductivity function (versus water content) for different soil types (after Freeze and Cherry, 1979).

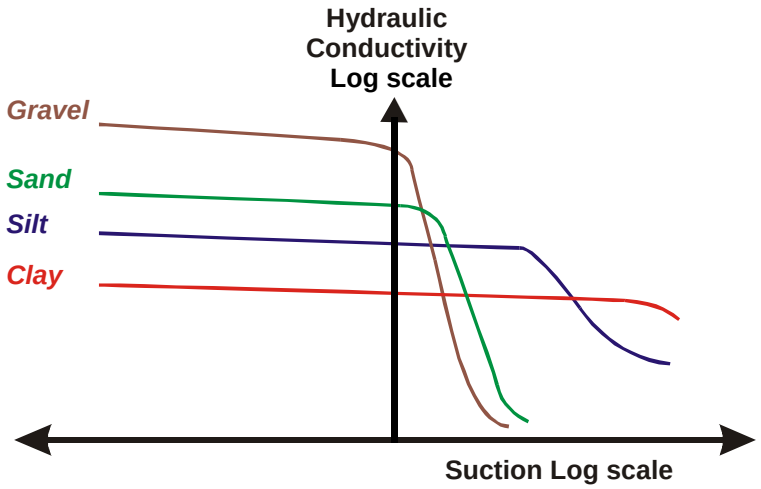

Figure 1.7 The hydraulic conductivity function (versus suction) for different soil types (after Freeze and Cherry, 1979).

1.2.2 Vapour Flow

Vapour flow dominates moisture movement once the residual moisture content is reached. Vapour diffusion occurs due to a gradient in vapour concentration as described by Fick's First Law:

$$q_v = -n_a D^* \frac{\partial C}{\partial x} \qquad [1.6]$$

where q_v is the diffusive mass flux of water vapour (kg/m^2/s), n_a is the air-filled porosity, D^* is the diffusion coefficient for water vapour(m^2/s), C is the concentration of water vapour (kg/m^3), and x is the dimension in direction of diffusion (m).

Vapour diffusion starts to predominate when the water content is sufficiently low that liquid water flow no longer occurs. This is thought to occur at a suction of approximately 3000 kPa (Wilson, 1990). Suction can be related thermodynamically to relative humidity as shown in Equation 1.7:

$$RH = e^{\left(-\psi \mu_v \upsilon_{w0}/RT\right)} \qquad [1.7]$$

where ψ is total suction (kPa), μ_v is molecular mass of water vapour (18.016 kg/kmol), ν_{w0} is the specific volume of water (inverse density) (m$_3$/kg), R is the universal gas constant (8.314 J/mol K), and T is the absolute temperature (K).

According to Equation 1.7, a suction of 3000 kPa corresponds to a relative humidity less than 100% (Wilson, 1990). This relationship simplifies the understanding of vapour flow, because vapour flow can only occur due to a vapour pressure gradient, and a vapour pressure gradient will only occur once the relative humidity has dropped below 100%.

1.3 Evaporation and Transpiration

Evapotranspiration is comprised of two components, evaporation and transpiration both of which may influence the moisture condition in unsaturated soils. Evaporation is an abiotic process occurring due to a vapour pressure gradient between the soil and the atmosphere. Transpiration is a biotic process that refers to the uptake and subsequent release of moisture into the atmosphere by plants.

1.3.1 Evaporation

The potential evaporation is the maximum rate at which water can evaporation from a soil surface and is only a function of climate. The evaporation rate will decrease as the soil surface becomes unsaturated and soil conditions will become the dominant factor controlling evaporation (Koliasev, 1941).

Potential evaporation can be measured directly using evaporation pans (Maidment, 1993), or calculated based on air temperature, relative humidity, wind speed, and solar radiation (net radiation) (Penman, 1948). Additional methods to calculate potential evaporation include the Thornthwaite method (1948), the Priestley-Taylor Model (1972), and the Complimentary Relationship (Bouchet, 1963).

A word of caution is necessary regarding the use of an evaporation pan to characterize evaporation at a site. Various types of pans are available such as sunken pans, floating pans, and surface pans. The most common pan is the surface-type pan such as the Class A evaporation pan (Maidment, 1993). Gray (1970) observed that a Class A evaporation pan overestimated the cumulative potential evaporation from a large fresh water reservoir near Weyburn, Saskatchewan by 1.25 times over a 6 month period. The difference was attributed to advected energy and the influence of aridity as a result of the soil surrounding the evaporation pan.

It is important to note that a Class A evaporation pan does not provide a measure of actual evaporation either since the actual evaporative rate decreases as the soil profile restricts the movement of moisture to the surface as a result of increased soil suction. Therefore, the Class A evaporation pan does not provide a site specific measure of potential evaporation or actual evaporation and its accuracy in characterizing either parameters will be site specific and more than likely change on a day to day basis.

An example of this is shown in Figure 1.8 where the ratio of potential evaporation (calculated based on the Penman (1948) method using field data collected at a semi-arid tropical site) to pan evaporation (measured at the same site using a Class A evaporation pan) is shown on a daily and cumulative basis over two annual wet-dry cycles. The key point is that when an evaporation pan is used to measure potential evaporation, a pan coefficient is required to reduce the measured pan value to a potential evaporation value. In general, the person utilizing the data will assume a single pan coefficient for the site based on “experience” or on a selected value from the literature for similar

ground cover conditions. However, Figure 1.8 shows that it can be argued the pan coefficient changes on a daily basis, likely due to a number of factors, and definitively shows that the pan coefficient changes on a seasonal basis.

A misunderstanding with respect to the fundamental processes of unsaturated flow sometimes leads to a misuse of evaporation during cover system design and seepage potential. The misunderstanding is based on the fact that actual evaporation from a soil surface will not equal the potential evaporation. For example, there are numerous mining operations where annual rainfall is significantly less than potential evaporation. The broad classification of these sites as “dry sites” is often useful when comparing relative seepage from a waste storage facility to a site where rainfall exceeds potential evaporation on an annual basis (i.e. a “wet site”). However, these broad classifications cannot be used to estimate the water balance for the sites and determine net percolation for a cover system. For example, if rainfall at the dry site was 500 mm per year and potential evaporation was 1,500 mm, one cannot conclude that the net loss will be 1,000 mm of water, nor can it be assumed that net percolation from the cover system to the underlying waste will be zero.

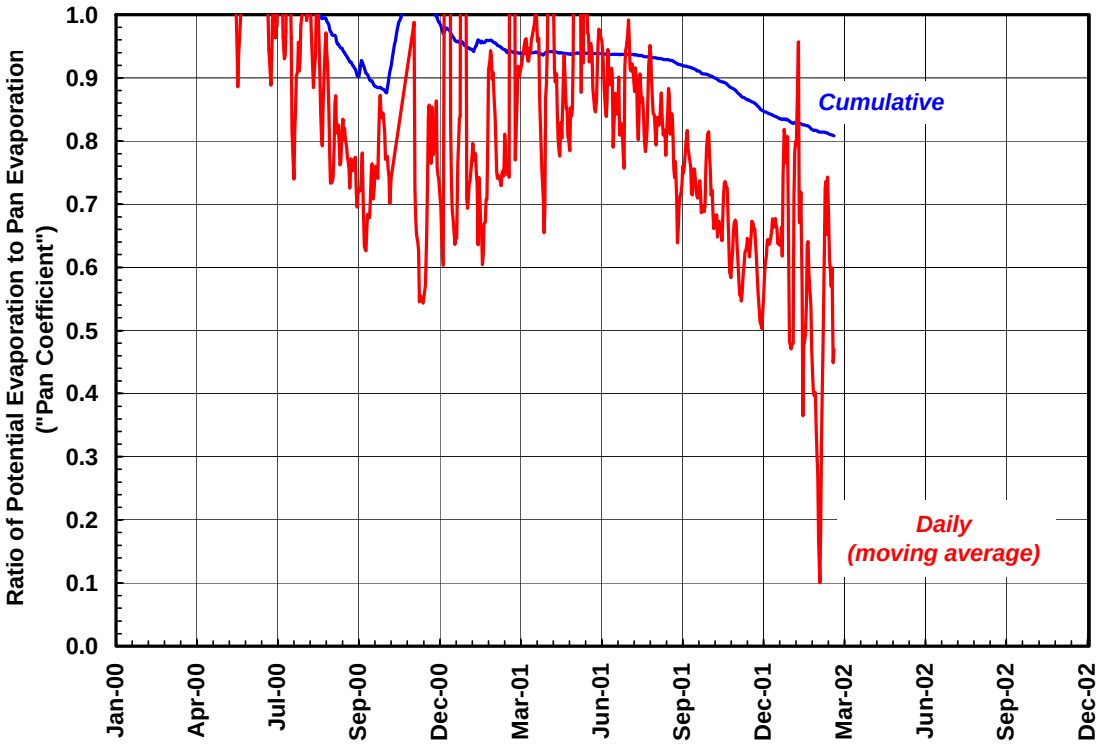

Figure 1.8 Daily and cumulative pan coefficient for a semi-arid tropical site (CANMET, 2002).

Soil can sustain evaporation rates equal to potential evaporation rates for only short periods of time. Wilson *et al.* (1994) conducted a column test using an initially saturated soil where the soil evaporated at a rate close to the potential rate for only a few days, as shown in Figure 1.9. The evaporation rate quickly dropped to rates less than ten percent of the potential rate once the soil surface began to dry. The Wilson *et al.* (1994) laboratory data shown in Figure 1.9 follows the classical curve of evaporation from soils as discussed by Hillel (1980).

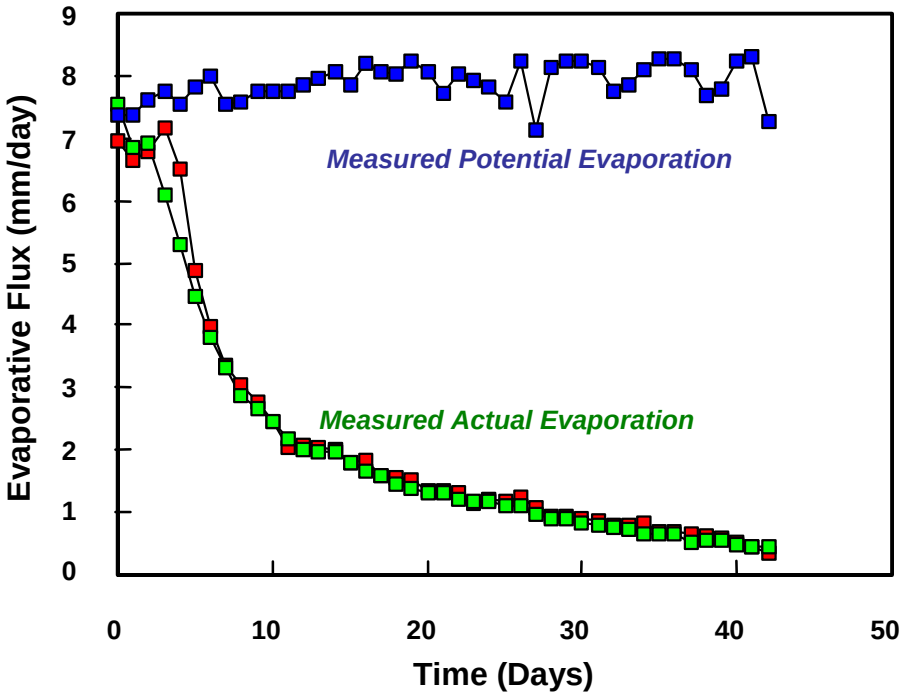

Figure 1.9 Evaporation from an unsaturated soil (after Wilson *et al.*, 1994).

It should be noted that potential evaporation is a function of atmospheric conditions only (i.e. not dependent on soil conditions). In general, soil will evaporate at the potential rate as long as the soil remains saturated at the surface, or there is a phreatic surface relatively close to the surface (e.g. a bare tailings surface in close proximity to the edge of the tailings pond).

The relative influence of the various measurements will change depending on whether the soil cover system is evaporating at a potential rate or at the actual evaporative rate. For example, Swanson (1995) observed during a sensitivity analysis of climate parameters for the soil cover system at Equity Silver Mine in British Columbia, that increasing wind speed caused an increase in evaporation from a saturated soil surface. However, if the soil surface was unsaturated, a lower wind speed caused an increase in evaporation. Swanson (1995) concluded that under dry conditions high wind speeds cooled the surface resulting in a lower surface vapour pressure, which reduced the actual evaporative rate. When the cooling effect of wind is not present the surface temperatures can

get very high, resulting in increased vapour migration toward the surface (Swanson, 1995). Quantifying potential and actual evaporation on a site specific basis is paramount since overestimating evaporation will underrate the ability of a soil cover system to perform as an oxygen barrier and overestimate its ability to function as a water infiltration barrier.

1.3.2 Transpiration

Plant transpiration is a result of root uptake within the soil profile and is a function of potential evaporation, the degree of plant development (Richardson and Ritchie, 1973), and soil suction (Wilson, 1990). Potential plant transpiration increases non-linearly with increases in the green leaf area index (Swanson, 1995). The green leaf area index is defined as the ratio of the total green leaf area per unit area of ground surface. When the soil profile begins to dry out, vegetation begins to be stressed and transpiration decreases from the potential rate. Plant transpiration shuts down completely once the wilting point has been reached. The wilting point refers to the soil suction at which the plant can no longer extract water, typically taken as 1,500 kPa (Fredlund and Rahardjo, 1993). It should be noted however that the suction conditions corresponding to the plant limiting and wilting points are not well known for the majority of vegetation species native to most if not all mine site locations. The role of transpiration in terms of cover system performance will be addressed in subsequent sections of this manual.

1.4 Oxygen Transport

Oxygen within the root zone is indispensable to plant growth and is of major importance for soil organisms and soil chemical processes. Oxygen can also move across the surface of mine waste by diffusion and advection processes in both the gas and solution phases. Diffusion is the movement of molecules or ions from a region of higher concentration to one of lower concentration as a result of random Brownian movement. An advective process is one in which the solute (i.e. dissolved oxygen) is carried along with a moving solvent (i.e. infiltrating water). In the case of oxygen transport into waste rock, the oxygen may be carried along with air moving through the pile. Therefore, oxygen can be transported across the cover system as a result of infiltrating water containing dissolved oxygen, through barometric pumping, wind action, and volume displacement during infiltration, all coupled with diffusion within both the liquid and gas phase.

Following cover placement, the predominant mode of oxygen transport across the cover and into the mine waste is through diffusion. The rate of diffusion is described through the use of Fick's Law, presented in Equation 1.8 for vapour diffusion and written as follows for oxygen diffusion:

$$q = -n_{eq} D^* \frac{\partial C}{\partial x} \qquad [1.8]$$

where q is the mass flux of oxygen (kg/m^2/s), n_{eq} is the equivalent porosity, D^* is the diffusion coefficient (m^2/s), C is the oxygen concentration in the gas phase (kg/m^3), and x is the depth (m). The equivalent porosity, which defines the porosity available for oxygen movement, is described in detail in Aubertin *et al.* (2000). The diffusion coefficient through a dry soil is nearly four orders of magnitude higher than it would be for a saturated soil, which is similar to the coefficient of diffusion through water. A tension saturated cover material consequently acts much like a "blanket of water" held in place by the cover material itself. Figure 1.10 illustrates the effect of the degree of saturation of a soil on the diffusion coefficient of oxygen. There is a substantial decrease in the oxygen diffusion coefficient at higher degrees of saturation. However, if cracks and / or macropores develop in the cover system, which extend from the surface of the capping material to the underlying material, oxygen ingress in those areas will likely be governed by transport through the air-filled macropores and cracks, depending on the number of cracks. In this case dissolved oxygen concentration in the water within the soil matrix at the air / water interface is a function of the oxygen concentration in the air-filled macropores or cracks.

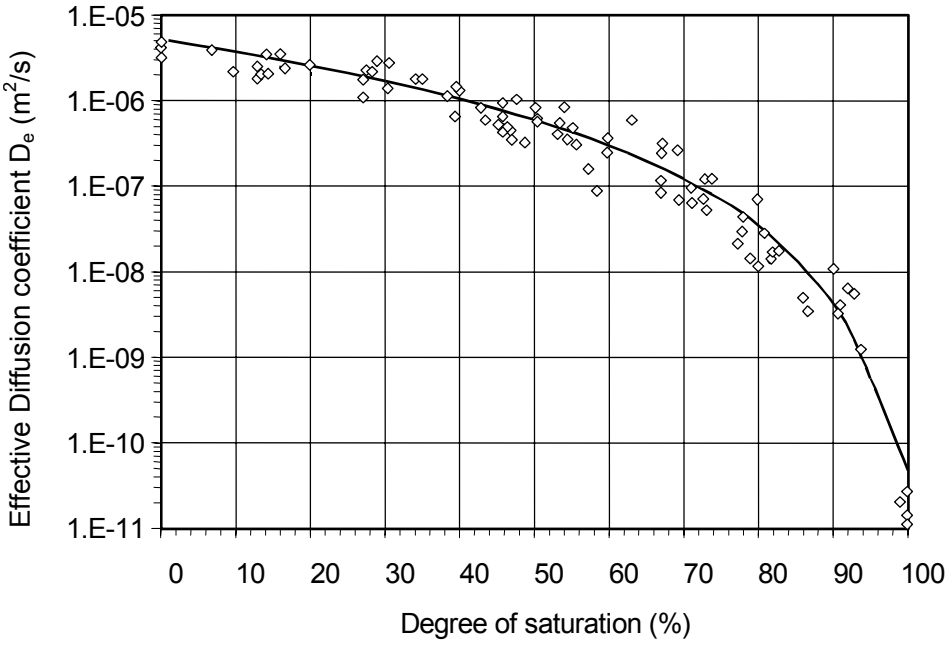

Figure 1.10 Effect of the degree of saturation on the oxygen diffusion coefficient, where $D_e = n_{eq}D^*$ (Mbonimpa *et al*., 2003). Note, the curve is based on a model, and is not a best-fit of the data points.

2 APPLICATIONS OF THEORY TO COVER DESIGN

The design of cover systems requires the application of the theory introduced in the previous section. This section introduces application of the theory to flow issues important to cover design such as bypass flow, cover storage capacity, capillary barriers, and oxygen ingress.

2.1 Flow Issues

There are a number of issues related to flow that are important to understand when designing a cover system. Following is a discussion on bypass flow, basal inflow, wetting, and pore-water velocity.

2.1.1 Bypass Flow

An understanding for bypass flow under unsaturated conditions is required to understand the capillary barrier concept utilized in cover system design. Bypass flow through vertical columns of segregated soil is described in this section. Capillary barriers are introduced in the following section.

The predominant pathway for fluid flow in an unsaturated soil is strongly influenced by heterogeneity in the profile, coupled with the specific flow condition being considered. The reason for this is that the "most permeable" pathway is not always through the same material as it would be in a saturated soil. The most permeable pathway in an unsaturated profile may be the coarser or finer soil, depending on the range of suction or degree of saturation that develops.

The general term "bypass flow" is used to describe flow non-uniformity due to profile heterogeneity. In such cases, the flow is channelled through the more conductive regions, or "preferred" flow paths. Structural non-uniformity within mine waste occurs commonly due to variability in the nature of waste material as a result of segregation during mining, stockpiling, and placement activities. When moisture flows preferentially through a waste rock pile, pore-water quality is greatly influenced by the "preferred" flow path.

This counter-intuitive flow pattern occurs because the coarse-textured material is incapable of retaining water under higher values of matric suction. As water drains from the coarser material, it reaches residual levels of saturation in which liquid flow is increasingly restricted. Under the same levels of suction the finer textured material is capable of retaining water and therefore maintains a higher unsaturated hydraulic conductivity. This results in bypass flow occurring through the fine-textured layers rather than through the coarse layers.

To illustrate the concept of bypass flow in coarse and fine-textured material, consider a column of two materials, one coarser and one finer textured, vertically segregated, but with no barrier to flow between the materials, as shown schematically in Figure 2.1. The fundamental physical law describing the flow of water (i.e. Darcy's Law) states that water flow occurs due to differences in hydraulic head (i.e. water flows from high hydraulic head to low hydraulic head).

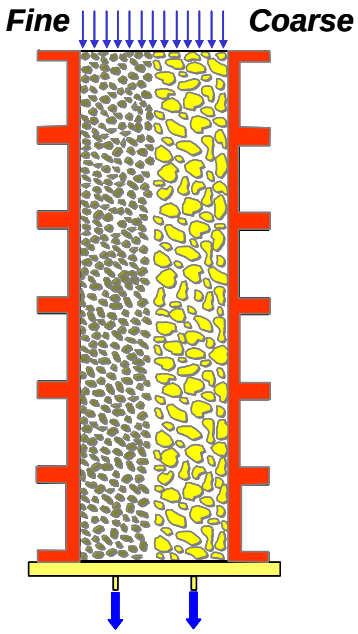

Figure 2.1 Schematic of a column with segregated coarse and fine-textured materials (O'Kane *et al.*, 1999).

Figure 2.2 shows the particle size distribution curves (a) and the hydraulic conductivity functions (b) for the coarser and finer textured materials shown in Figure 2.1. The hydraulic conductivity functions of the two materials cross at a matric suction of approximately 1 kPa, as shown in Figure 2.2. At suctions greater than the 1 kPa the finer material has a higher hydraulic conductivity and becomes the preferred flow path. Water is applied to the top of the column as shown and the question arises: Will the water "prefer" to flow in the finer or coarser textured material? Clearly, for saturated conditions the preferred flow path will be the coarser material due to its higher hydraulic conductivity. However, the correct answer to the question for unsaturated conditions, such as that within a covered waste rock pile, is: "It depends on the applied flux rate at the top of the column". In general, at low flux rates the "preferred" flow path will be the finer textured material. This counter-intuitive phenomenon of unsaturated zone hydrology has a significant impact on the hydraulic performance of segregated finer and coarser textured material, whether the material is separated as shown in Figure 2.1 or layered at an angle as would be found in a waste rock pile.

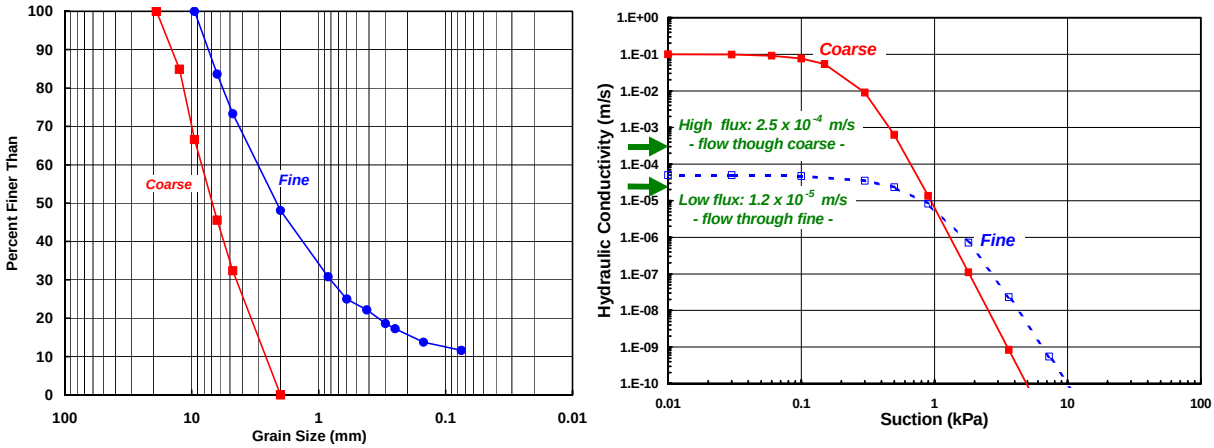

Figure 2.2 a) Particle size distribution and b) hydraulic conductivity function for the coarse and fine-textured materials shown in Figure 2.1 (O'Kane *et al.*, 1999).

The answer to the question of the preferred flow path for the water applied to the top of the column shown in Figure 2.1 can now be answered with some understanding. A flux rate applied to the top of the column that is greater than the saturated hydraulic conductivity of the finer textured material (see Figure 2.2b) will lead to bypass flow in the coarser material. The higher applied flux rate will create a pressure profile leading to saturation conditions where the effective hydraulic conductivity of the coarser material is greater than the finer material. Applied flux rates less than the saturated hydraulic conductivity of the finer textured material (see Figure 2.2b) will lead to bypass flow in the finer textured material. The lower applied flux rate creates a pressure profile where the coarser material drains while the finer material retains moisture and a higher hydraulic conductivity. The key issue is that determining the predominant flow path is not completely intuitive.

Figure 2.3 summarizes the percentage of flow conducted to each side of the column in lab experiments conducted by O'Kane Consultants Inc. (2000). It is evident that the percentage of the total water flowing through the finer material drops as the application rate increases, even though a limited number of column tests were conducted. As the application rate approaches the saturated hydraulic conductivity of the finer material, the percentage of the total flow occurring through the finer material drops rapidly. Essentially all flow is through the coarser material at fluxes above this value. Bypass flow can exist in a number of forms, three of which are described below.

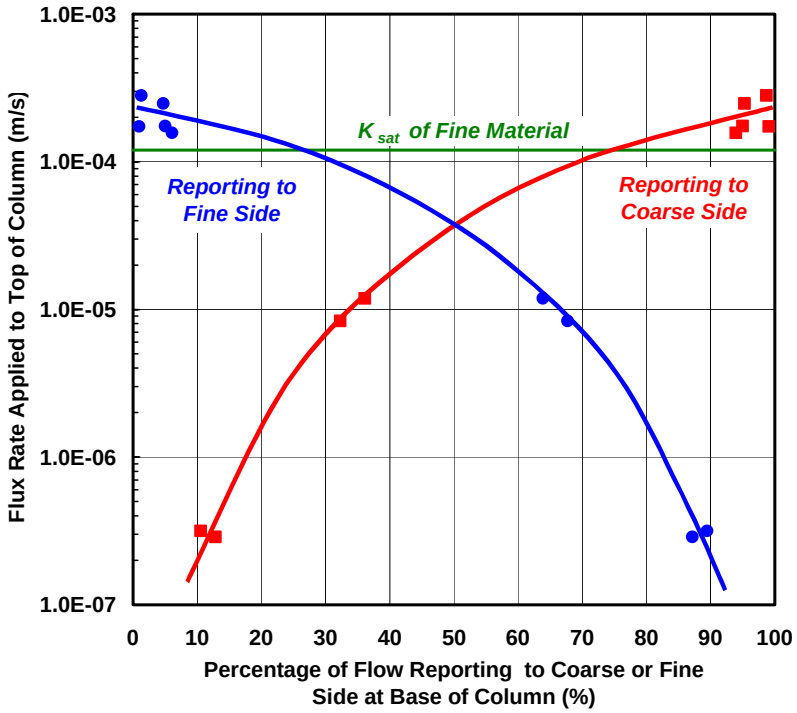

Figure 2.3 Percent of total applied water exiting column from both fine and coarse materials over the range of applied surface fluxes (OKC, 2000).

2.1.1.1 Funnel Flow:

In soil profiles that contain distinct layers of different textured materials, water preferentially flows through the more permeable layers. This form of bypass flow is referred to as funnel flow. Layers of steeply dipping coarse-textured, fine-textured, and well-graded layers form naturally during waste rock pile construction making them particularly susceptible to funnel flow conditions. In cases of funnel flow the preferred flow path is typically thought of as being the coarser textured material. However, due to its larger and more continuous pores this is not always the case. Under low rainfall and uncovered conditions, and certainly for covered waste rock conditions, it is possible for the finer textured soil to be more conductive and thus be the preferred flow path.

2.1.1.2 Macro-Pore Flow:

“Macro-pore flow” or “short-circuiting” are common descriptions given to bypass flow through the larger pores of a given media. As flow rate increases, higher fractions of the total flow are diverted to ever-larger channels. At high saturation almost all the flow (above 96%) is within “macro-pores”; pores larger than 0.2 mm in diameter (Scooter, 1978). Even modest increases in the rate of surface infiltration for uncovered waste rock conditions can lead to significant short-circuiting.

2.1.1.3 Fingering:

An unstable front or interface may develop when one fluid displaces another fluid of different density and / or viscosity, which leads to propagation of discrete fingers rather than a uniform surface. This form of bypass flow, referred to as "fingering", can occur in the heap leaching industry as leach solution infiltrates into the heap. Generally speaking, gravitational forces, heterogeneity, and low-conductivity layers promote fingering, while capillary forces have a stabilizing effect. Fingering most commonly develops at the interface of a coarse material overlain by a fine layer when ponding occurs above the fine layer. Heterogeneous soils under relatively high application rates are also prone to unstable wetting. Of significance with respect to fingering flow is the fact that after infiltration ceases and the profile drains, subsequent infiltration follows the same finger-like pathways which where developed in the initial infiltration (Stephens, 1996; Glass, 1991).

2.1.2 Basal Inflow

The issue of basal flow was discussed in the summary volume (Volume 1). Detailed discussion on this subject is outside the scope of this manual. The key issue is that the potential influence of basal inflow from groundwater and/or ephemeral surface water on the effluent seepage from waste rock and tailings storage facilities is often overlooked. An understanding of the potential impact of basal flow on mine waste decommissioning can be developed using conventional hydrogeologic theory and methods. Readers are encouraged to utilize the services of professional consultants with expertise in these assessments.

2.1.3 Wetting

During a rainfall or snowmelt event, water infiltrating into a cover can contribute to storage (ie. wetting) and may or may not result in percolation through the cover. The process of wetting is fundamental to predict net percolation rates as well as prediction of the available water holding capacity of a soil for use by vegetation.

The storage capacity of a soil is also known as the "field capacity" of the soil. The term "field capacity" has resulted in a significant amount of confusion due to the simplified definition provided for the term. Field capacity is often defined as the moisture content of a soil at 33 kPa of negative pore-water pressure, which implies that field capacity is a fixed value for a particular soil type (note that for soils known to be coarser textured, a value of 10 kPa is often used). However, field capacity depends on the infiltration rate as well as the soil type. Field capacity can also be defined as the water content of an infinitely deep profile after completion of drainage, but not at a hydrostatic condition.

The Kisch (1959) solution can be used to illustrate how there is a significant difference in suction profiles and water content profiles in uniform soil profiles under different, but small, steady state flux rates. This solution does not account for layering of different materials, which would alter the water

content profiles significantly. The following example, taken from Swanson and O'Kane (1999) is intended as a simplistic example to illustrate wetting.

Figure 2.4 shows a 20 m high column of silty sand, with an initial volumetric water content of 0.05. The infiltration rate applied to the surface is approximately 25 mm per year ($\approx$ 1 x 10^{-7} cm/s). The question is: when will water begin to seep from the base of the column of silty sand?

It is possible that water will seep immediately under the applied infiltration depending in the initial moisture content of the silty sand. However, if seepage did occur it would not be the water that infiltrated, but rather the water displaced from the bottom of the column as a result of the infiltration. To determine whether the sand will drain or wet in response to infiltration, the initial hydraulic state of the sand should be determined from the SWCC and the k-function, which are shown in Figure 2.5 for this example.

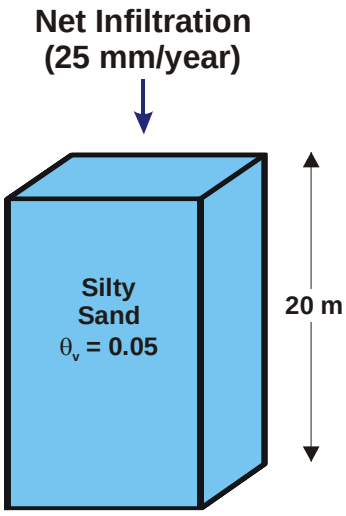

Figure 2.4 Example column of sand to illustrate wetting of an unsaturated soil.

The initial moisture content of the sand is 0.05, and is plotted on the SWCC shown in Figure 2.5. The hydraulic conductivity of the sand corresponding to this moisture content is approximately 1 x 10^{-13} cm/s shown in the k-function in Figure 2.5. The hydraulic conductivity at high suctions, especially at suctions greater than the residual water content, is difficult to predict, and therefore the function in Figure 2.5 is an approximation. The sand will prefer to come to equilibrium with the rate at which the water is infiltrating at the surface (i.e. 1 x 10^{-7} cm/s), and the hydraulic conductivity of the sand will be equal to the infiltration rate at this equilibrium condition. The volumetric water content at a hydraulic conductivity of approximately 1 x 10^{-7} cm/s is approximately 0.11. Therefore, the column of sand will have a propensity to wet, and the wetting front will advance through the sand column at a volumetric moisture content equal to 0.11, assuming the wetting front is abrupt. This is a reasonable assumption for a coarse-textured material, but less for a fine-textured material because it would retain

moisture at high suction conditions, and would thus possess a higher hydraulic conductivity beneath the wetting front.

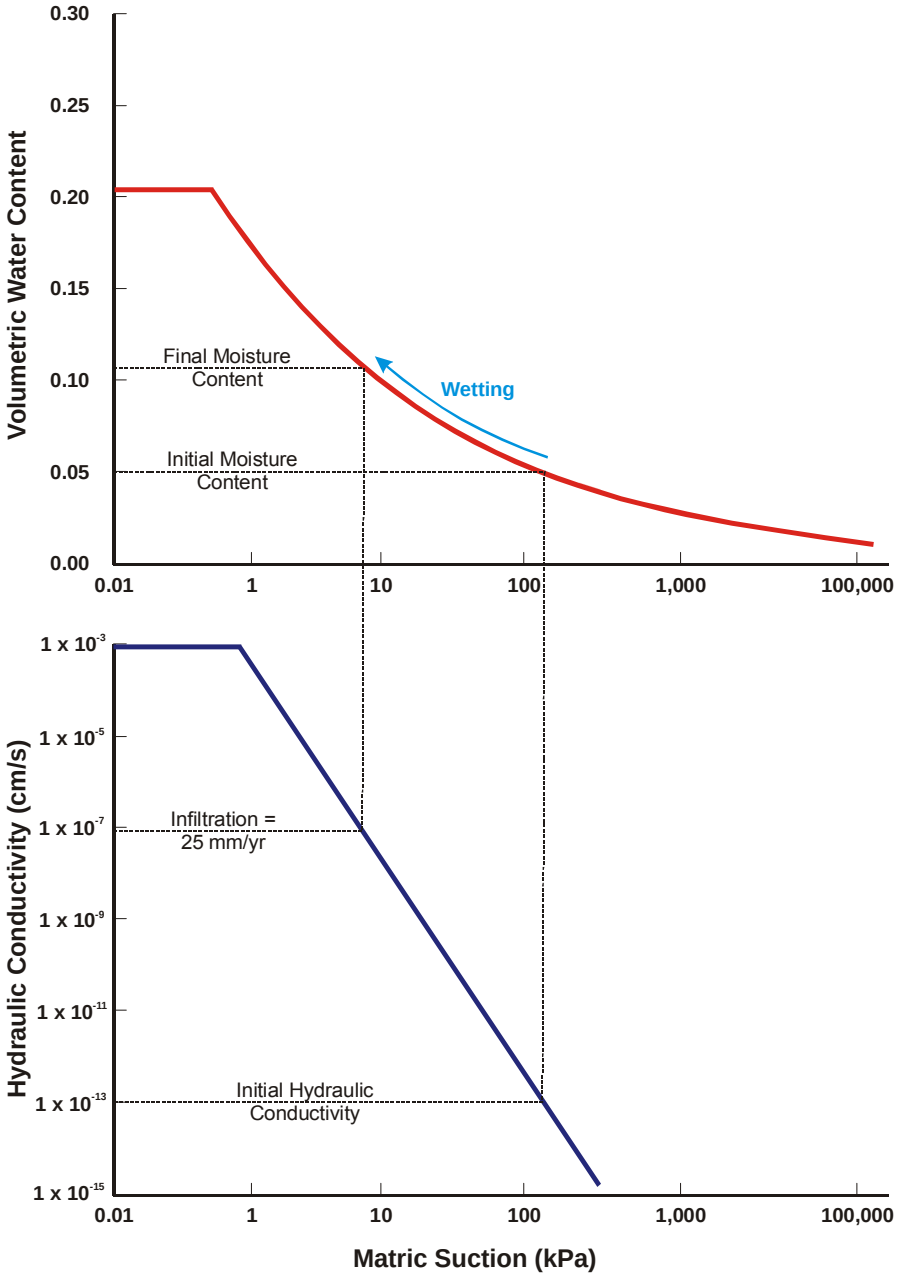

Figure 2.5 Estimating moisture contents from the soil water characteristic curve and hydraulic conductivity function.

2.1.4 Pore-Water Velocity

It is a common misconception to assume that infiltration in waste material beneath a cover system is equal to the velocity of pore-water migrating through the material. However, this is not the case

because pore-water velocity must account for the cross-sectional area available for water flow. Actual pore-water velocity is the ratio of the infiltration rate to the volumetric moisture content (Guymon, 1994). For example, if the net infiltration rate within the waste material was 25 mm per year and the volumetric waste content was 0.10, the average pore water velocity would be equal to 250 mm per year.

The pore-water velocity would equal the net infiltration rate if the there were no soil particles or air voids (i.e. an open column of water), and the space was completely filled with water. However, water flow in soils only occurs through pathways already filled with water as determined by the suction conditions. Therefore the effective porosity must be used to calculate the actual pore-water velocity.

2.2 Storage

2.2.1 Storage Capacity Calculation

Moisture store-and-release covers function by storing infiltration for a sufficient length of time so that the moisture can be removed by evapotranspiration. Therefore, the moisture storage capacity of the cover is a critical parameter in the design of a cover system to meet the specific infiltration requirements. The following example illustrates the calculation of the maximum storage capacity of a moisture store-and-release cover assuming no net percolation through the cover.

Figure 2.6 illustrates a 1 m moisture store-and-release cover over waste rock along with the SWCC's for both the cover and the waste material. The maximum storage capacity is the volume of water that the cover can hold between the "driest" and the "wettest" condition that will be encountered. Even under high evaporative demand, soils retain residual moisture content ("driest" condition). In the other extreme, waste rock piles tend to be well above the water table, and even under a relatively high infiltration rate, are unlikely to ever reach full saturation ("wettest" condition).

The "driest" condition (*Minimum* θ_w) for this example is assumed to be the water content of the cover material at 1500 kPa, which represents the permanent wilting point for vegetation. At suctions greater than 1500 kPa, most moisture transport is due to vapour diffusion, and as a result very little moisture is removed for large increases in suction. Therefore, this is a reasonable estimate of the "driest" condition.

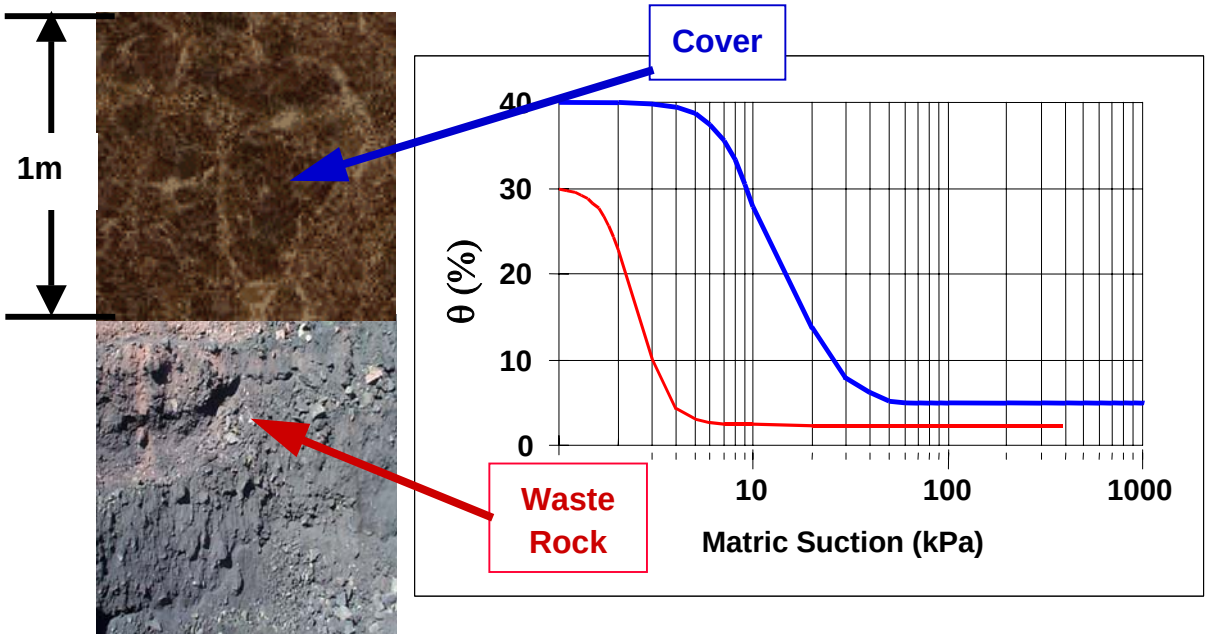

Figure 2.6 Schematic representation of a 1 m moisture store-and-release cover over waste rock with the corresponding SWCC for each material.

The assumed "wettest" condition (*Maximum* θ_w) is close to fully saturated and represents the moisture content after snowmelt or a significant rainfall event. Under hydrostatic conditions, this water content condition would vary through the cover profile, with wetter conditions at the bottom and drier conditions towards the surface. Figure 2.7 illustrates the profiles of the maximum and minimum water content with depth.

The difference between the maximum water content and the minimum water content is the maximum storage capacity of the cover. The difference can be estimated by dividing the cover into thin layers and estimating the water content in each layer.

For example, if the cover is divided into layers 0.1 m thick, the top layer can be estimated to have an average maximum water content of 35% and an average minimum water content of 5%. This results in a total storage capacity of 25 mm. If the remainder of the cover is estimated this way, the total storage in the 1 m moisture store-and-release cover is 335 mm (Figure 2.8).

For additional information on calculating storage capacity, the reader is referred to Morris and Stormont (1997).

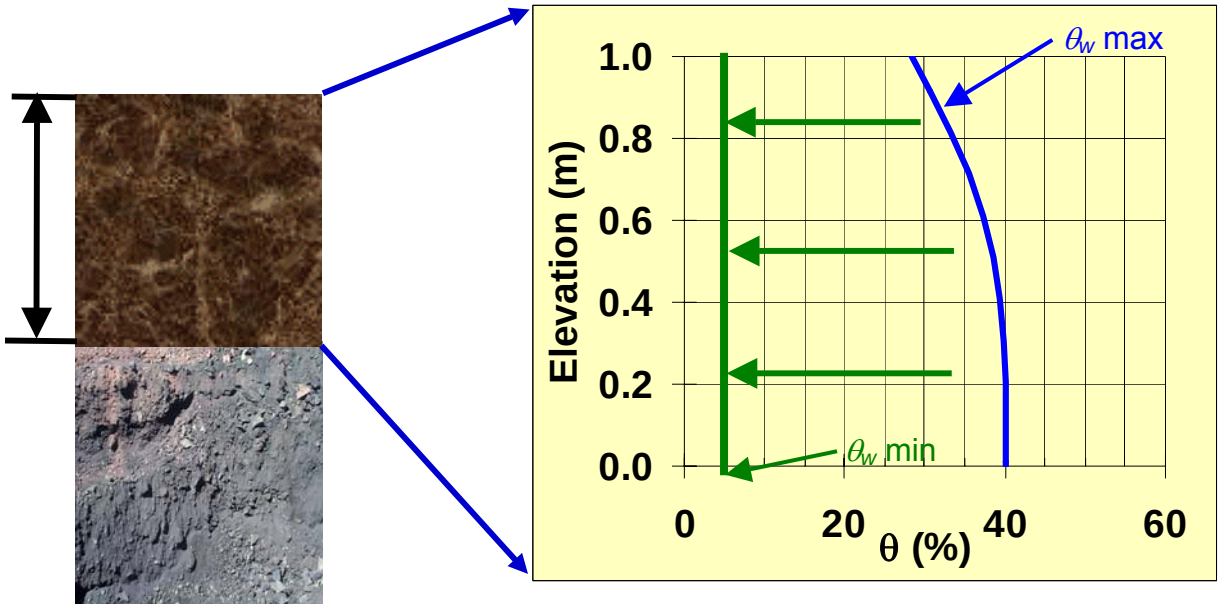

Figure 2.7 Schematic representation of a 1 m moisture store-and-release cover showing the maximum and minimum water content profiles.

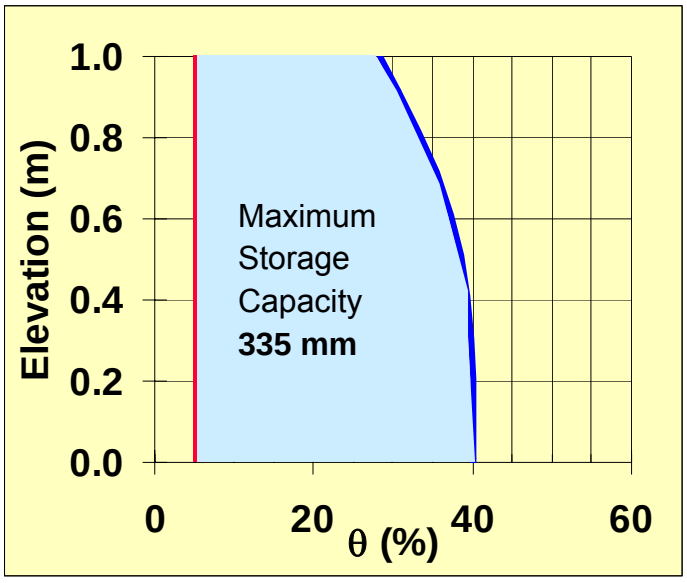

Figure 2.8 Shaded area illustrates the difference between the maximum water content and the minimum water content, which represents the maximum storage capacity.

2.3 Capillary Barriers

The capillary barrier concept is commonly used in the design of cover systems and more specifically, the design of multi-layer cover systems. Rasmusson and Erikson (1986), Nicholson *et al.* (1989),

Morel-Seytoux (1992), MEND 2.22.2a, Aubertin *et al.* (1996), Bussière and Aubertin (1999), and others describe the capillary barrier concept in detail.

A capillary barrier results when a finer textured material overlays a coarser textured material, as illustrated in Figure 2.9. The design of a capillary barrier is dependent on the contrast between the hydraulic properties of both the coarse and fine-textured materials. Figure 2.10 illustrates an example of contrasting material properties for two materials that could be used to form a capillary barrier. Capillary barriers, unlike compacted barriers, do not rely solely on low hydraulic conductivity to restrict movement into underlying material. Processes that increase hydraulic conductivity, such as desiccation andfreeze / -thaw, do not necessarily decrease the effectiveness of a capillary barrier.

Figure 2.9 Multi-layer cover system over waste material.

The lower coarser textured material may drain to a residual moisture content if conditions allow (see water content of sand at 20 kPa in Figure 2.10a). The residual suction for coarser textured material is relatively low. The overlying finer-textured material will not drain at this low suction and as a result, it remains in a tension saturated condition (see water content of silt at 20 kPa in Figure 2.10a). This “capillary” break will occur during drainage whenever the residual suction of the lower coarser textured material is less than the AEV of the upper finer textured material. The hydraulic conductivity of the coarser textured layer also drops many orders of magnitude at a residual moisture content compared to a fully saturated condition (by 20 kPa, the hydraulic conductivity of the sand is 4 orders of magnitude less than the silt as shown in Figure 2.10b)

A coarser textured layer overlying a finer textured layer may also be included in the design of a capillary barrier system but the role of this coarser layer is simply to prevent evaporation from the finer textured layer. The upper coarser textured layer may also reduce runoff, if the intensity is not too extreme, because it provides for storage of water following infiltration; thereby, allowing some water to reach the underlying finer textured material and satisfy any antecedent moisture losses.

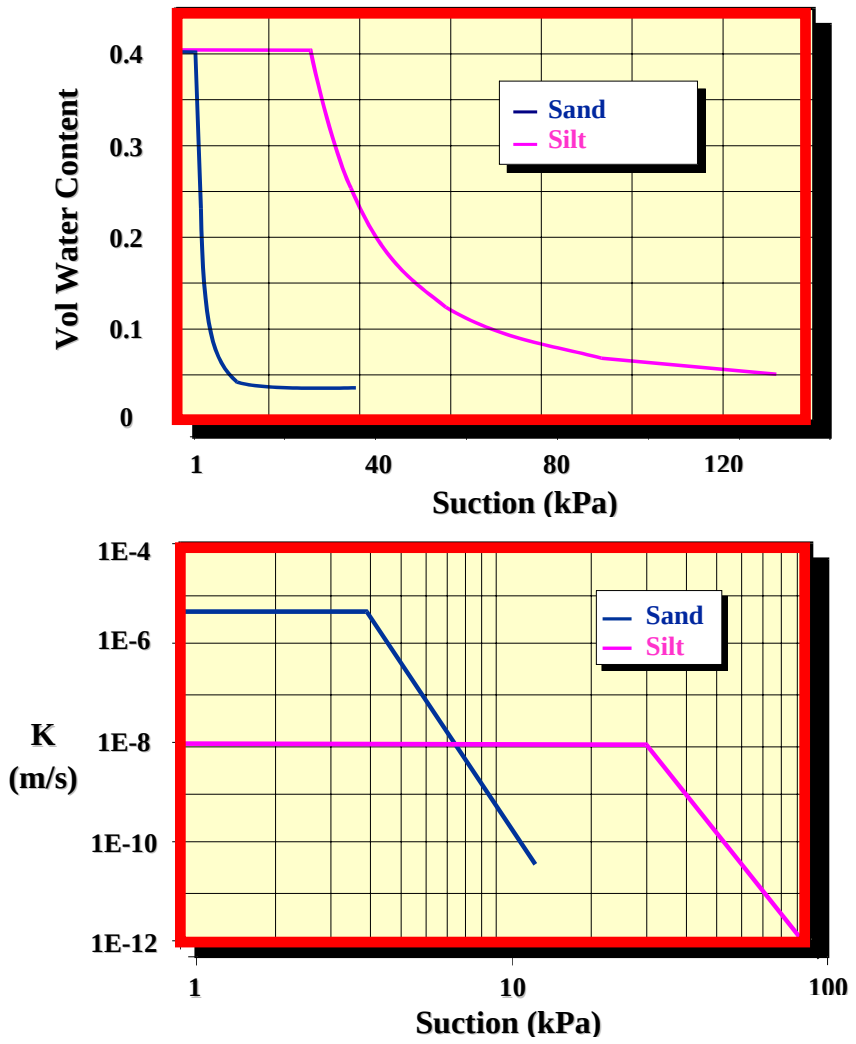

Figure 2.10 Hydraulic conductivity function (a) and SWCC (b) illustrating the contrast in hydraulic properties between a sand and a silt. Note the suction scales are different.

In summary, the capillary barrier concept is utilized in the design of cover systems for two primary reasons. The first is to maintain near-saturation conditions within a central, finer textured layer under all climatic conditions. This in turn limits the ingress of oxygen as described in the next section. In addition, the lower hydraulic conductivity of the finer textured layer (usually compacted), combined with the lower capillary barrier, provides a control on net percolation to the underlying waste material. Capillary barriers are considered as an alternative in arid and semi-arid climates where maintaining a layer within the cover system at high saturation conditions (i.e. a compacted layer) may not be possible. Capillary barriers also act to restrict the upward capillary rise of salts and/or oxidation products from underlying waste material into the finer textured cover material, which in turn could have a detrimental impact on vegetation.

2.3.1 Cover Systems on a Sloping Surface

Considerable fundamental and applied research has been undertaken on the performance of cover systems for mine waste rock and tailings. In general, the literature illustrates that the majority of cover designs deal with one-dimensional flow of heat and moisture vertically across horizontal layers. Field performance monitoring has also typically focused on one-dimensional performance. In reality, sloping surfaces are relatively common in the reclamation of waste rock surfaces or tailings dam walls. The hydraulic performance of a cover system placed on these slopes, and its ability to function as oxygen ingress and water infiltration control systems, will be different than that predicted by idealized one-dimensional numerical models (Boldt-Leppin *et al.*, 1999).

The topographically controlled groundwater flow system developed in fine-textured soils in waste piles is analogous to natural groundwater flow on hill slopes. The distribution of the hydraulic heads is controlled by the topography because when different elevations of cover material are at similar pressures as a result of soil-atmosphere moisture fluxes, an elevation gradient still exists down slope. The flow system is mainly influenced by low hydraulic gradients controlled by the slope, low hydraulic conductivity, high capillary forces due to the fine-textured soils, and spatial homogeneity (Barbour *et al.*, 1993). The effect of these factors in controlling the groundwater flow system is shown in Figure 2.11.

Figure 2.11a demonstrates that the water table remains near the surface if the combination of hydraulic conductivity, surface flux, and topographic slope is properly chosen, even under low infiltration rates (Fig. 2.11b) and steepened slopes (Fig. 2.11d). Increases in the hydraulic conductivity (Fig. 2.11c), or heterogeneity in the soil (Fig. 2.11e) will produce lower water tables or increase the rate of seepage.

Figure 2.12 is a schematic illustration of the components of a hill slope hydrologic cycle. It is clear from Figure 2.12 that side slopes of waste rock piles are analogous to natural hill slopes. A significant amount of research that could be applied to waste rock cover systems has been completed studying the hydrology of natural hill slopes (Boldt-Leppin *et al.*, 1999).

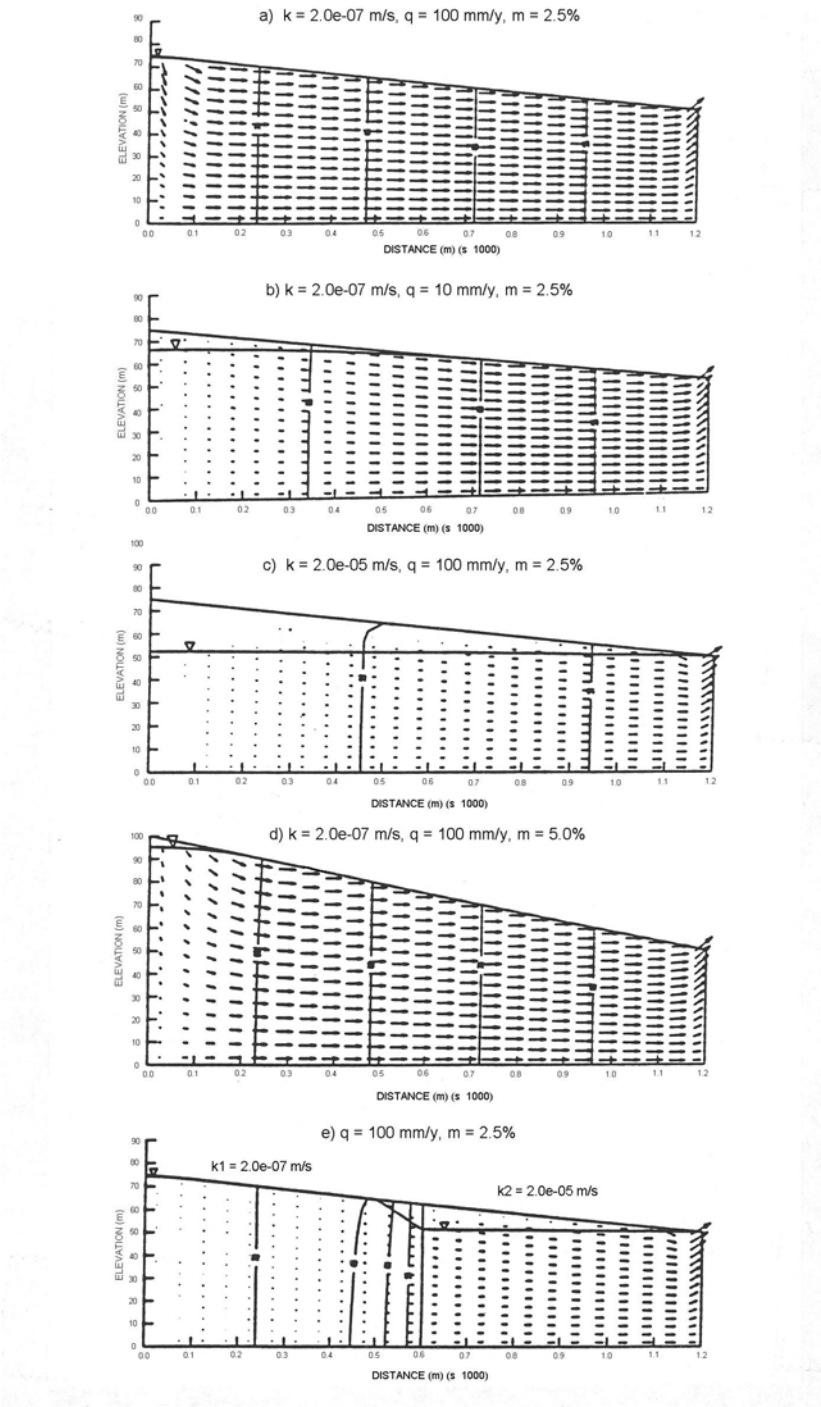

Figure 2.11 Effect of changes in hydraulic conductivity (*k*), climatic flux to the soil surface (*q*) and topographic slope (*m*) on the groundwater flow system (after Barbour *et al.*, 1993).

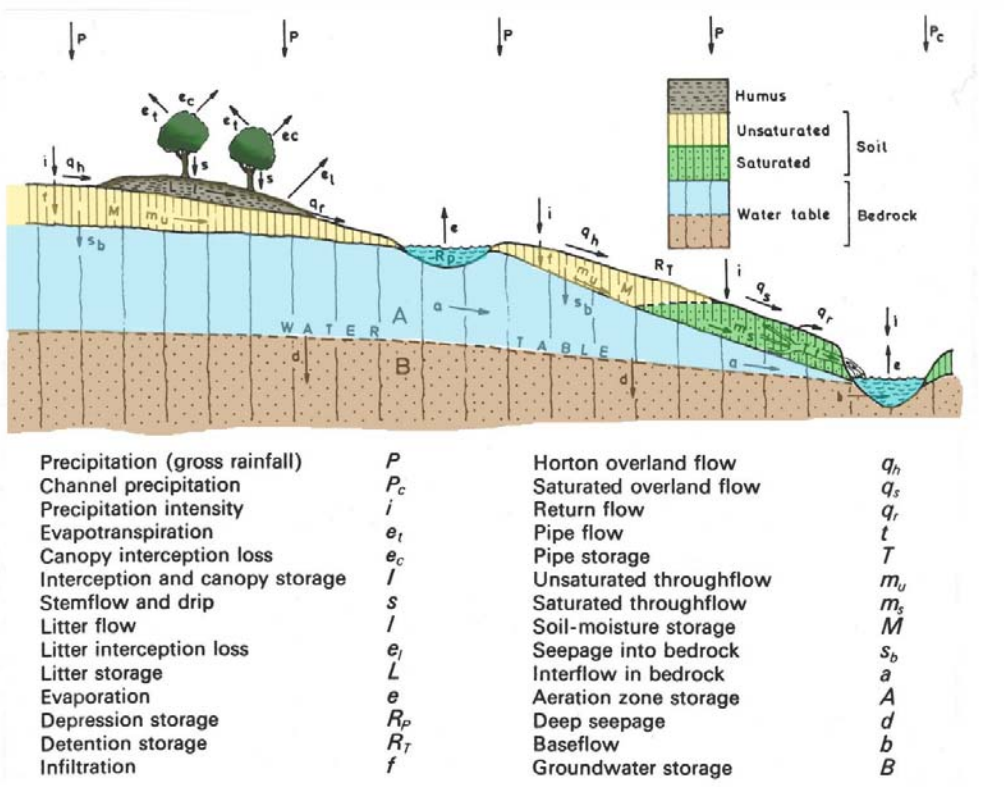

Precipitation (gross rainfall)	P	Horton overland flow	q_h
Channel precipitation	P_c	Saturated overland flow	q_s
Precipitation intensity	i	Return flow	q_r
Evapotranspiration	e_t	Pipe flow	t
Canopy interception loss	e_c	Pipe storage	T
Interception and canopy storage	I	Unsaturated throughflow	m_u
Stemflow and drip	s	Saturated throughflow	m_s
Litter flow	l	Soil-moisture storage	M
Litter interception loss	e_l	Seepage into bedrock	s_b
Litter storage	L	Interflow in bedrock	a
Evaporation	e	Aeration zone storage	A
Depression storage	R_P	Deep seepage	d
Detention storage	R_T	Baseflow	b
Infiltration	f	Groundwater storage	B

Figure 2.12 Components of the hill slope hydrologic cycle (from Chorley, 1978).

Bussière *et al.* (2003) evaluated the effect of geometry (specifically slope and slope length) on the behaviour of capillary barrier covers designed to reduce oxygen transport. A combination of laboratory results, field-scale results, and two-dimensional modelling results were presented. Figure 2.13 illustrates SEEP/W modelling results for a capillary barrier cover consisting of silt sandwiched between two sand layers. The slope was 3H:1V with a 50 m slope length. The results of the modelling showed that the upslope parts of the cover desaturated more than the downslope parts of the cover. Modelling using coarser materials with steeper slopes showed greater desaturation upslope.

Whipkey and Kirkby (1978) provide another example of the influence of a sloping surface on cover system performance. Their analysis illustrates the development of sub-surface lateral flow along a slope with infiltration occurring along the surface. The authors show that in a two-layered system (bottom layer less permeable than top layer under saturated conditions), under steady rainfall, most of the moisture percolates through the impeding layer, whereas most of the lateral flow occurs in the permeable layer, as shown schematically in Figure 2.14.

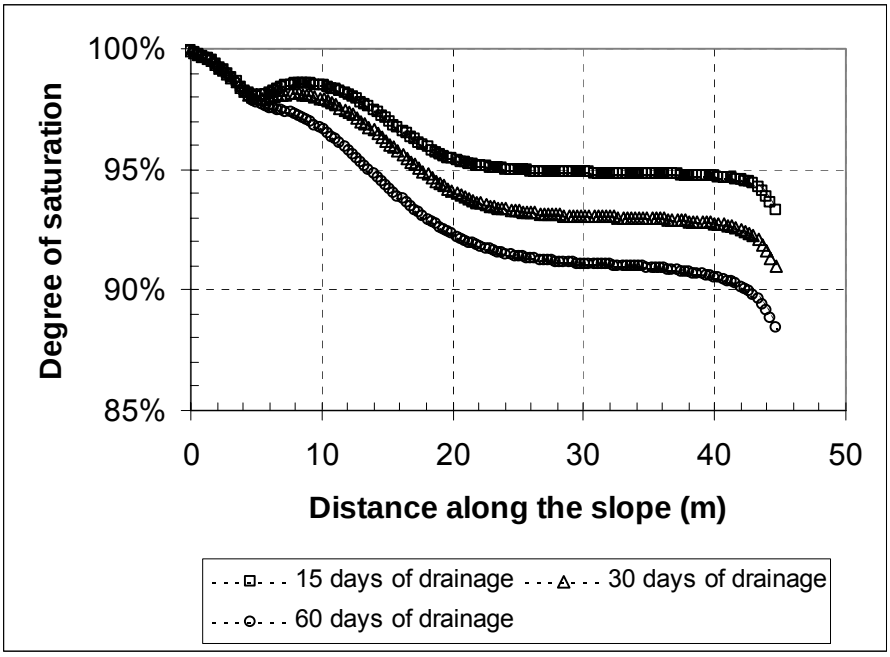

Figure 2.13 Modelling results illustrating the effect of slope length (0 = bottom of the slope) on the degree of saturation in the center (mid-depth) of the moisture-retaining layer of a capillary barrier cover (Bussière *et al*. (2003)).

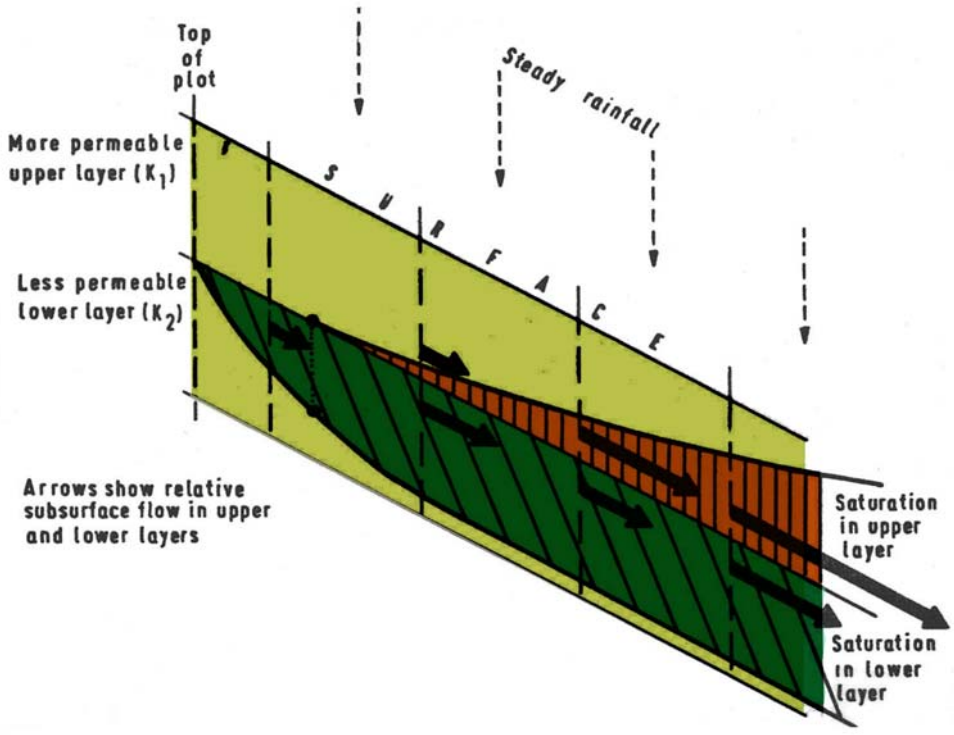

Figure 2.14 Saturated layers and subsurface flow above and below the contact with an impeding layer, under conditions of steady rainfall (after Whipkey and Kirkby, 1978).

2.3.2 Capillary Barrier Diversion Lengths on Sloping Surfaces

The proper arrangement of an unsaturated fine-textured soil overlying an unsaturated coarser soil on a sloping contact can divert infiltrating water away from the coarser soil (Ross, 1990). Under unsaturated conditions the hydraulic conductivity of the coarser soil layers is greatly reduced and the higher hydraulic conductivity of the finer textured material allows it to become the preferential flow pathway. Under these conditions, water infiltrating into the soil profile will be transported laterally through the finer textured soil. Figure 2.15 shows the hydraulic conductivity functions for a finer and coarser textured material, which will form the basis for subsequent discussion on capillary barrier diversion length.

The use of soil diversion layers is founded on the concept of bypass flow. As water infiltrates into the fine-textured soil it is transported down the slope. At some point, sufficient water will collect in the fine-textured soil to reduce the negative pore-water pressures to the point where the unsaturated hydraulic conductivity of the finer soil is similar to that of the underlying coarser soil (Point h_w on Figure 2.15). The distance from the crest of the slope to this point is defined as the diversion length.

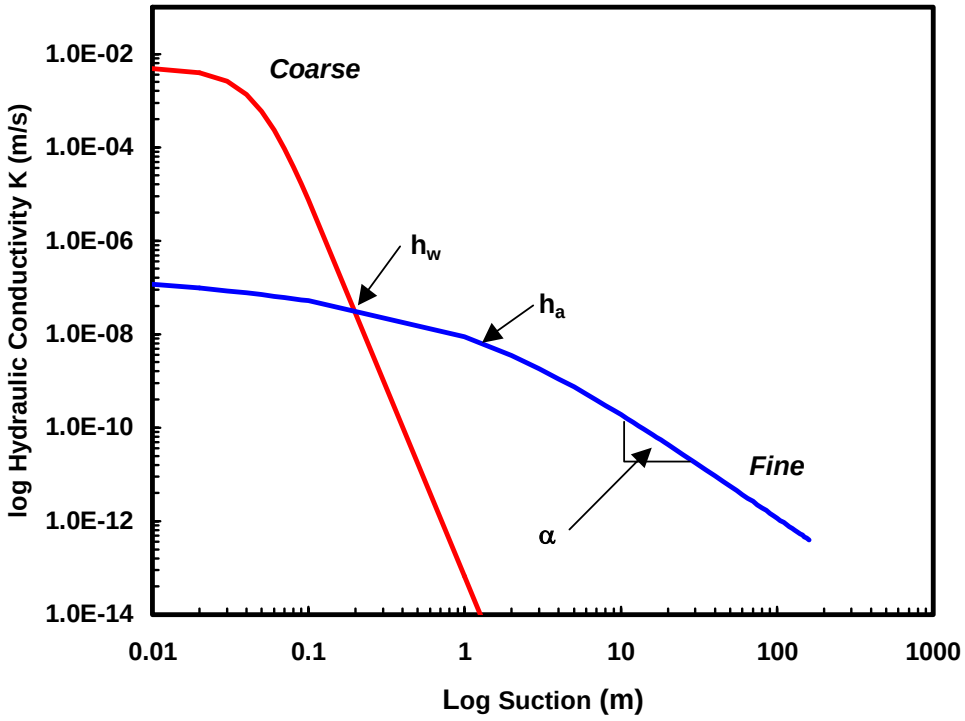

Figure 2.15 Hydraulic conductivity function for the coarse and fine-textured materials used in the capillary barrier diversion length example.

Relevant Research in the Area of Diversion Lengths:

Ross (1990) completed an analytical investigation of the diversion layer concept and presented a simplified equation to define the diversion length expected from a sloped capillary barrier.

$$L = \frac{K_s \cdot \tan\varphi}{q \cdot \alpha} \qquad [2.1]$$

where:

- L = diversion length (L),
- K_s = saturated hydraulic conductivity (fine material) ($L \cdot T^{-1}$),
- ϕ = slope angle (degrees),
- q = infiltration rate ($L \cdot T^{-1}$), and
- α = sorptivity index (L^{-1}).

The saturated hydraulic conductivity is a measurable geotechnical property of the finer textured soil material. The slope angle is controlled during construction and may be optimized to produce the most efficient cover design. The infiltration rate is an estimate of the long-term percolation through the fine-textured soil layer. The sorptivity index is a measure of the inverse slope of the straight-line portion of the hydraulic conductivity versus negative pore-water pressure curve (i.e. hydraulic conductivity function).

Steenhuis and Parlange (1991) suggest variations to the model presented in Equation 2.1. Since the sorptivity index is the slope of the hydraulic conductivity function, this value varies over the entire range of suction conditions, especially close to saturation. Steenhuis and Parlange (1991) present a variation to Equation 2.1 that includes terms representing the air entry value and the water entry value (suction at residual water content). This equation takes into account unstable flow theory.

Stormont (1996) tested two 7.0 m long, 1.2 m thick capillary barriers on a 10% slope. One test specimen had a homogenous finer textured layer while the other had two thin beds of fine sand placed within the finer layer. The homogenous capillary layer did not have the ability to divert infiltration across its 7.0 m length. However, the heterogeneous finer layer acted as a suitable diversion barrier. Stormont (1996) concluded that the ability of the finer textured layer to conduct water is the most important factor in the determination of diversion length.

Example Diversion Length Calculation:

The proper function of a capillary barrier system requires the removal of water from the system before it can be breached by high pore-water pressure resulting in flow through the coarse layer. The function of the cover system is often influenced by the ability of the finer textured soil to store water

during periods of high infiltration and release it back to the atmosphere as evaporation or evapotranspiration during dry periods. An additional option is to slope the capillary barrier layers so water is transmitted to the base of the slope for collection and drainage. In this case, the length of the slope must be regulated to ensure that the capillary barrier is not compromised before the water is diverted to the bottom of the slope. A calculation of the diversion length capacity of the capillary barrier must be completed.

Assume the top of the waste rock pile is approximately 300 m wide by 600 m long (Figure 2.16) and that the proposed closure design requires contouring of the pile surface to create gentle undulations across the width of the slope. The newly created slopes would drain to catchment ditches running the length of the waste rock pile. This system would collect runoff and infiltration water, channel it to one end of the top of the waste rock pile, and transport it to the base of the pile using engineered drop structures. Alternatively, the finer textured cover layer may be thickened at these locations to provide for greater moisture storage, potentially greater evapotranspiration, and continuing diversion of water downslope along the direction of the drainage swale.

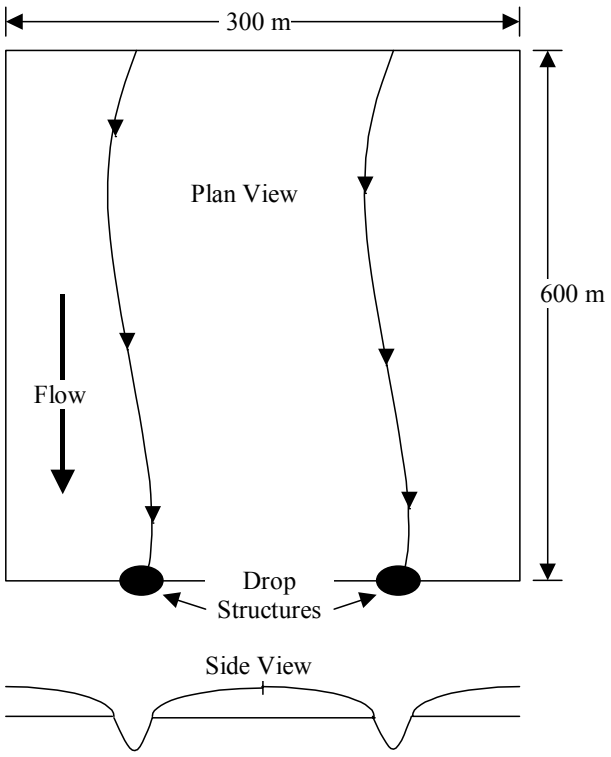

Figure 2.16 Plan and side views of the example waste rock pile upper surface showing contours and channels.

The advantages of utilizing the diversion length capacity of the contoured slopes are (Stormont, 1996):

1) to possibly reduce the thickness of the fine layer required to store all the expected precipitation;
2) to account for unusual climatic events which exceed the design storage capacity of the system; and
3) to provide a redundant component within the capillary break system.

In preparation of the cover system design, an analysis of the factors contributing to the diversion length capacity of the cover system is required. The diversion length of the finer textured soil is calculated from Equation 2.1. Table 2.1 details the expected diversion lengths for a moderate infiltration condition (50 mm/yr) with varying slope angles, finer textured layer hydraulic conductivity, and sorptivity indices.

Using Equation 2.1 with inputs of K_s = 5.0 x 10^{-7} m/s, ϕ = 5°, q = 1.58 x 10^{-9} m/s, and α = 0.34 m^{-1}, the diversion length of the capillary barrier system is calculated to be 9.49 m. This diversion length would require 15 channels running the length of the waste rock pile shown in Figure 2.16.

Table 2.1
Calculated diversion length capacity for the moderate infiltration case.

	Diversion Lengths (m)					
	Low K (k = 1x10^{-7} m/s)		**Mod. K (k = 5x10^{-7} m/s)**		**High K (k = 1x10^{-6} m/s)**	
Layer Inclination (°)	**Low Alpha (α = 0.34 m^{-1})**	**High Alpha (α = 0.42 m^{-1})**	**Low Alpha (α = 0.34 m^{-1})**	**High Alpha (α = 0.42 m^{-1})**	**Low Alpha (α = 0.34 m^{-1})**	**High Alpha (α = 0.42 m^{-1})**
3	1.14	1.36	5.69	6.82	11.4	13.6
5	1.90	2.28	9.49	11.4	19.0	22.8
8	3.00	3.66	15.2	18.3	30.5	36.6

The diversion lengths presented in Table 2.1 assume a constant hydraulic conductivity in the horizontal and vertical direction. However, in the case of soil profiles produced by constructing a cover system in lifts, the horizontal hydraulic conductivity is often higher than the vertical hydraulic conductivity. This anisotropy can increase the diversion length of capillary break layers. Stormont (1995) modified the general equation given by Ross (1990) to include anisotropy. The study concluded that the value calculated by Equation 2.1 can be multiplied by the factor of anisotropy

(K_h/K_v) to produce the revised diversion length. Stormont (1995) reported that the anisotropy factor of natural homogenous material is approximately four, constructed soil layers can be expected to have higher anisotropy factors.

To modify the diversion length calculation example cited above, a conservative estimate of the anisotropy (K_h/K_v = 2.0) would result in a doubling of the diversion length from 9.49 m to 19.0 m. This would decrease the number of required drainage channels from fifteen to eight. Recalculation with a high anisotropy ratio (K_h/K_v = 10) results in a diversion length of 94.9 m, requiring only two drainage channels.

2.4 Oxygen Ingress

Oxygen ingress is a key component evaluated during the design of a cover system. Numerical models as well as simplified analytical solutions can be used to qualitatively demonstrate the contribution to the annual total oxygen mass flux from the individual components contributing to oxygen ingress. These components include:

1) oxygen diffusion through the matrix pore-air;
2) oxygen diffusion through the matrix pore-water;
3) advection of dissolved oxygen with infiltrating water;
4) barometric pumping; and
5) the increase in oxygen available to the underlying material as a result of cracks that extend to the underlying material-capping material interface.

The following sections discuss the contributions of these five components to oxygen ingress.

2.4.1.1 Barometric Pumping – Soil Matrix

Oscillations in barometric pressure are both diurnal, corresponding to daily heating and cooling of the atmosphere, and seasonal, resulting from the passage of weather fronts. Note however, that it is these latter barometric pressure fluctuations that are of most concern with respect to oxygen ingress. A pressure gradient is imposed on the soil air. When the barometric pressure rises, fresh surface oxygen enriched air is driven into the soil; however, when the barometric pressure drops, oxygen depleted soil air vents upward into the atmosphere. Atmospheric pressure conditions should be analyzed over as large a representative period of years for a site as possible. The atmospheric conditions for a period from March 1998 to April 1998 are shown in Figure 2.17 for an example site, which are representative of the complete record of data not shown. Steep oxygen concentrations gradients are typically present in a soil matrix due to chemical and biological process combined with a low diffusion coefficient. This results in wide variability of oxygen concentrations in the “growth medium” soil matrix, which are strongly related to the soil structure.

Oxygen transport is restricted to diffusion and advection through the water phase in a saturated or tension-saturated matrix. The relationship between the relative coefficient of air permeability and degree of saturation is for practical purposes a “mirror image” to that of water permeability and the degree of saturation. This aspect of the relative permeability versus degree of saturation function is common in nearly all gas-liquid systems in porous media. The relative coefficients of diffusion for oxygen and water as a function of the degree of saturation are also explained by this inverse relationship.

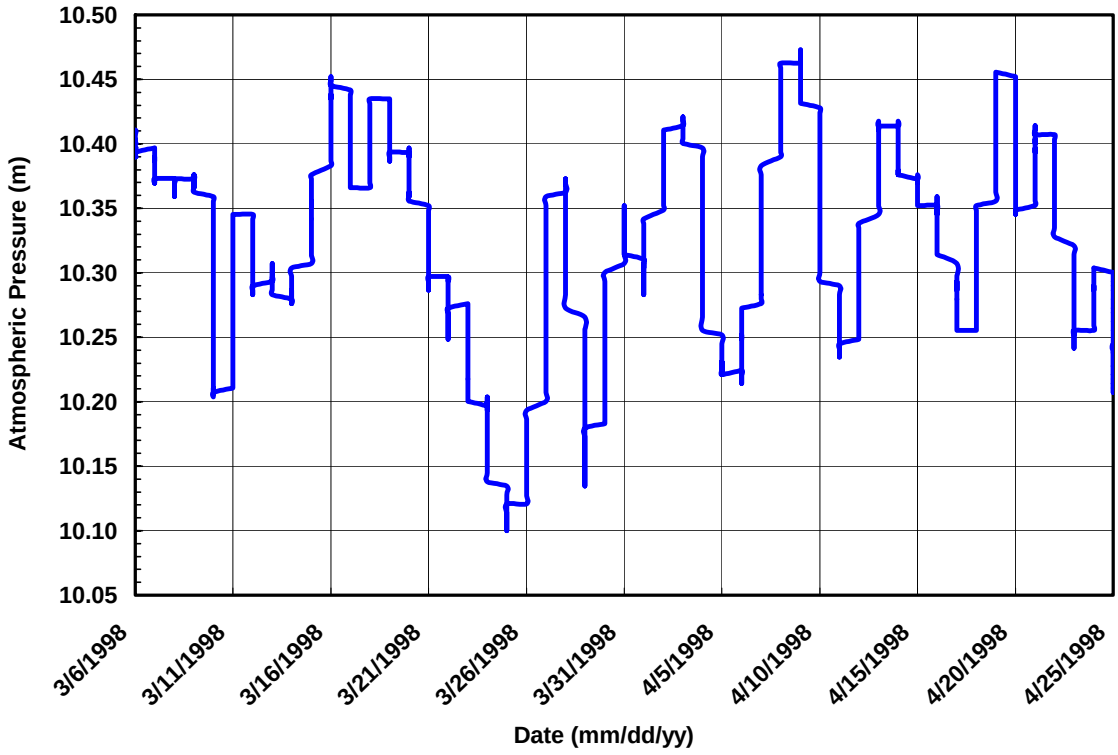

Figure 2.17 March 1998 and April 1998 atmospheric conditions for the example site.

The atmospheric pressure condition for the example site was analyzed for significant changes in atmospheric pressure conditions, which may drive barometric pumping. Generally, pressure changes lasting less than a day were considered insignificant after analyzing the data for this particular site. The trend indicated that the majority of pressure gradients lasted more than one day. Atmospheric pressure conditions are summarized in Figures 2.18 and 2.19. Figure 2.18 indicates the frequency of specific pressure gradient ranges, while Figure 2.19 presents the duration that the pressure gradients were imposed.

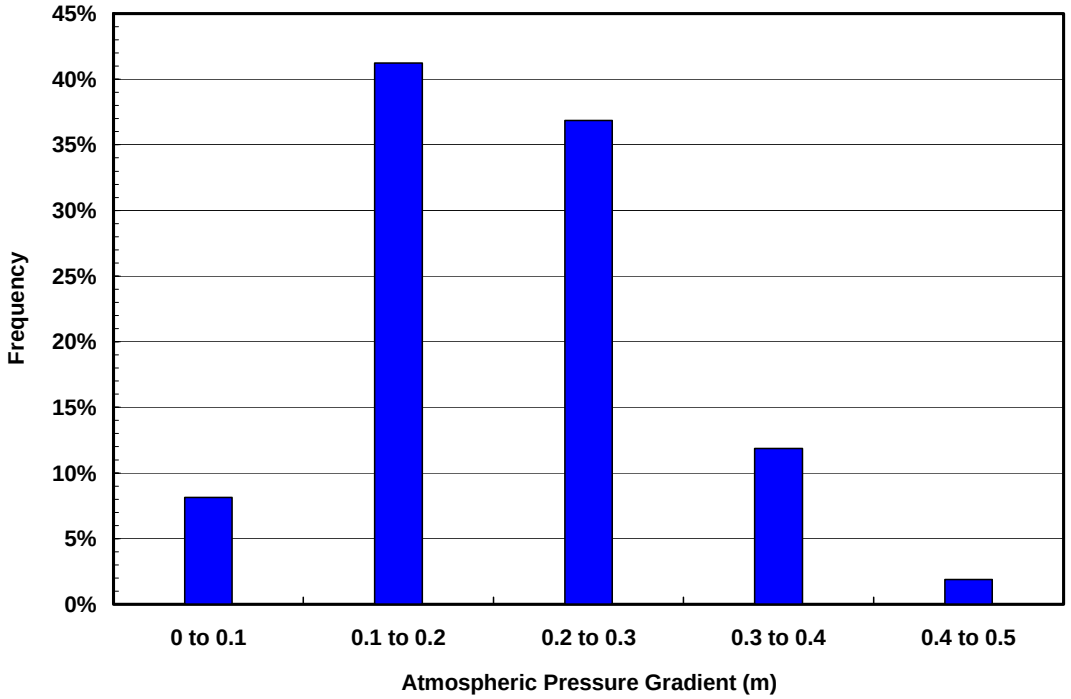

Figure 2.18 Frequency of the atmospheric pressure gradients imposed on the cover pore-air space.

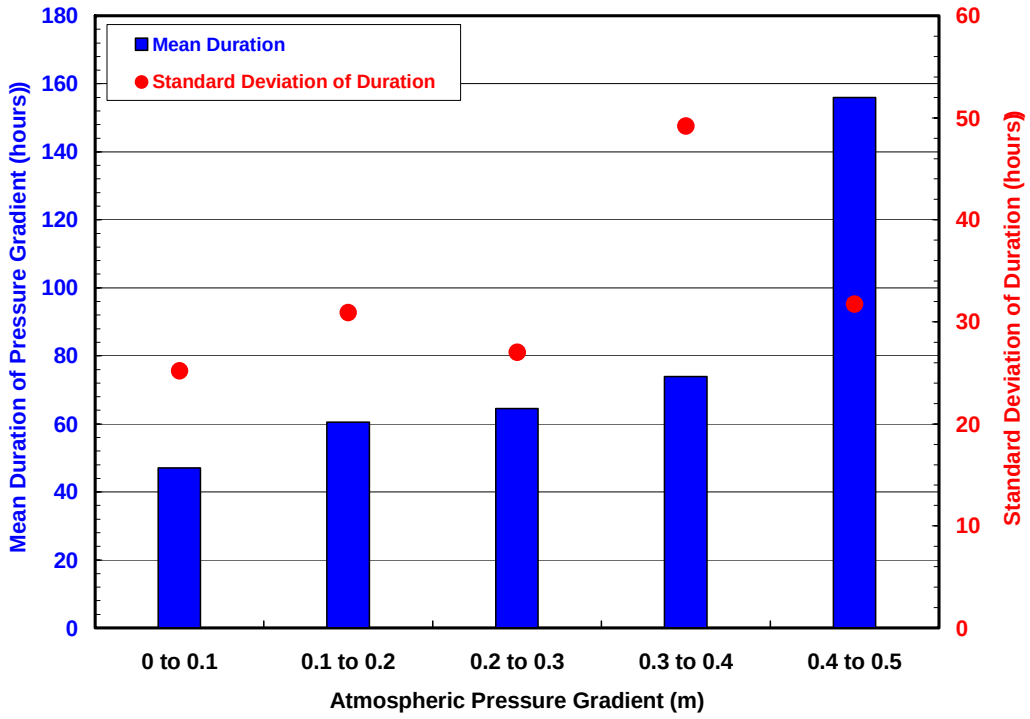

Figure 2.19 Duration of the atmospheric pressure gradients imposed on the cover pore-air space.

The total movement of soil air is dependent primarily on the magnitude and period of the pressure oscillations, the soil permeability to air, and depth to an impermeable boundary. This boundary can be the water table, bedrock, or extensive layers of low permeability material. Changes in atmospheric pressure on a daily basis are generally small, thus the overall soil air displacement is also small (with an estimated range of centimetres to metres). Typically, no net soil air displacement occurs in a homogeneous medium due to barometric-induced advective forces alone.

The flow characteristics of air moving through a soil must be determined to evaluate the effects of barometric pumping. The coefficient of water permeability of a rock, sediment, or soil is the ability to permit fluid to flow through it. The coefficient of water permeability is also referred to as the hydraulic conductivity. More precisely, the coefficient of water permeability is the volume flow rate of water through a unit cross-sectional area of a porous medium under the influence of a hydraulic gradient of unity, at a specified temperature. The magnitude of the coefficient of permeability depends on the properties of both the fluid and the medium. An alternative measurement of a porous medium is the intrinsic permeability, which depends on the properties of the rock, sediment, or soil alone. The saturated hydraulic conductivity as a function of the intrinsic water permeability is expressed as:

$$K = \frac{\rho_w * g}{\mu_w} k \qquad [2.2]$$

where:

K = saturated hydraulic conductivity (m/s),

ρ_w = fluid density (water) (kg/m^3),

μ_w = absolute viscosity of water (kg/m s), and

k = intrinsic permeability of the soil (m^2).

Values of intrinsic water permeability were calculated for all cover and tailing materials for the example site, based on the measured coefficient of water permeability, the fluid properties of water, and Equation 2.2. The coefficient of air permeability can be calculated based on the intrinsic permeability, the fluid properties of air, and Equation 2.2, as per Fredlund and Rahardjo (1993).

The coefficient of air permeability is not a constant for an unsaturated soil, but rather is a function of the degree of saturation. A change in air permeability for a soil will occur as a result of a change in the availability of pores available for flow, that being the portion of pores not occupied by water.

Semi-empirical equations are used for obtaining the coefficient of air permeability versus the degree of saturation. These semi-empirical equations are based on the pore size distribution and the soil water characteristic curve (SWCC). The coefficient of air permeability as a function of the degree of saturation can be determined as (Fredlund and Rahardjo, 1993):

$$K_a = K_d (1 - S_e)^2 (1 - S_e^{((2+\lambda)/\lambda)}) \quad [2.3]$$

where:

K_a = coefficient of air permeability at a given effective degree of saturation (m/s),

K_d = coefficient of air permeability with respect to the air phase for a soil at a degree of saturation equal to zero (m/s),

S_e = effective degree of saturation = $(S - S_r)/(1 - S_r)$ where S_r is residual degree of saturation, and

λ = pore size distribution index.

Barometric pumping is based on the oscillation of atmospheric pressure conditions in relation to the soil pore air pressure. An increase in atmospheric pressure drives air into the soil while a decrease leads to soil venting. The effects of barometric pumping take on a piston-like flow in homogenous soils, moving up and down with changing pressure conditions. Based on the behaviour of airflow moving into the cover system, penetration of the "piston" must exceed the cover thickness for oxygen-enriched air to enter the underlying material.

In the example, a compacted cover layer was evaluated with respect to the penetration depth of oxygen enriched atmospheric air by barometric pumping. This represents a worst-case scenario as the atmospheric conditions are assumed at the compacted layer surface rather than at the actual surface of the overlying growth medium, approximately 1 metre above the top of the compacted layer. The example results presented are for a warm climate and therefore the reduction of oxygen flux during freezing conditions was not evaluated.

Ranges of atmospheric pressure gradients were imposed on the compacted layer for the mean duration of the pressure gradient applied, as per Figure 2.19. The penetration depths at degrees of saturation equal to 0%, 25%, 50%, and 85% are shown in Figure 2.20. It is only the largest atmospheric pressure gradient (i.e. 0.4 – 0.5 m) at 0% degree of saturation, which allows oxygen to reach to the depth of the underlying waste material. This calculation assumes that the applied gradient is imposed instantaneously, which is not the case in reality, and also ignores the fact that the same pressure gradient is also applied half the time in a manner to vent the internal gases. Both of these assumptions result in an oxygen flux greater than would actually occur. Furthermore, based on the atmospheric conditions observed for 1997 and 1998, a pressure gradient of 0.4 - 0.5 m occurs at a frequency of approximately 2% in relation to the remaining pressure gradients. In summary, for the conditions as presented in the example, a negligible mass of oxygen will likely ingress across the tension-saturated cover system to the underlying material as a result of barometric pumping. This conclusion may be different for a cover system with differing conditions, and would definitely be different for an uncovered waste rock surface where oxygen ingress as a result of barometric pumping is common. However, the key point is that the example provides a simple analytical method for evaluating the potential for barometric pumping to result in an increase in oxygen ingress.

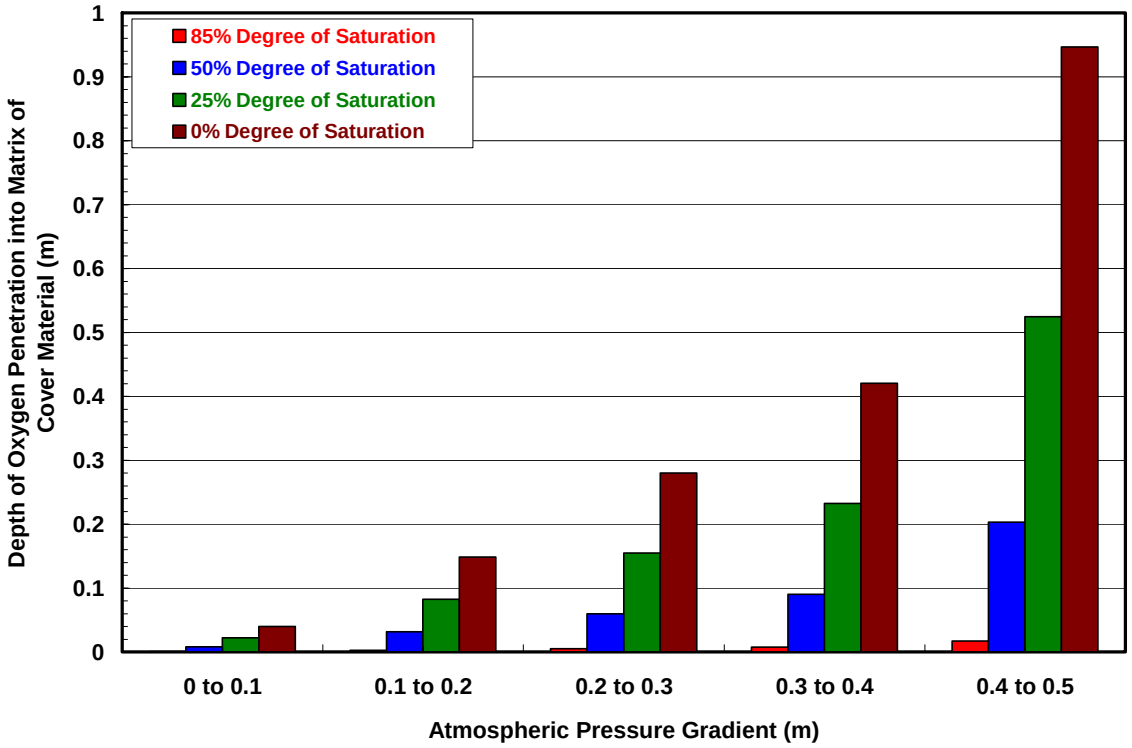

Figure 2.20 Penetration depth of oxygen enriched atmospheric air into the compacted layer at degrees of saturation of 0%, 25%, 50% and 80% (atmospheric conditions are assumed at the compacted layer surface).

2.4.1.2 Barometric Pumping – Presence of Cracks

In general, cracking of a soil cover material can occur in a variety of ways, ranging from desiccation triggered by extended droughts and transpiration, to structural failures of the cover material due to settlement and lateral mass movement. Typically, desiccation cracks are widest at the surface and decrease to a point at depth. A crack formed as a result of structural failures would likely have the same crack width at surface to depth since these cracks are formed in part by lateral movement. The crack geometry evaluated for in this example was assumed to be the worst case, characteristic of a lateral movement and not desiccation. The example site cover system was evaluated on the basis of the ratio of the area of openings created by the cracks to the entire cover surface. In addition, it was assumed that the cracks would exist for the entire year, in order to compare the maximum influence on oxygen ingress due to the cracks. Note that it is unlikely these cracks would be allowed to exist for an extended period of time because their presence would be noted during inspection following a large magnitude earthquake or stability failure, and they would be repaired.

It should also be noted that the potential for cracks to develop such that atmospheric conditions would exist at the surface of the underlying waste material is considered to be minimal. Cover systems in

general are not rigid, because they are designed with the potential to accommodate stresses that are reasonably expected to occur at a site. At certain sites the potential for displacement in a large magnitude earthquake does exist, and the cover system must be designed to be able to withstand a small amount of displacement in these settings. However, as with other engineered structures, inspection following such a large event should occur.

Atmospheric conditions were assumed to exist at the base of the underlying material at the base of the crack for the example. The mass of oxygen entering the underlying waste material, tailings in this example, over a range of saturated moisture contents for various crack percentages are shown in Figure 2.21. In all cases atmospheric air enters the tailings material because the cracks were assumed to expose tailings.

A secondary analysis can be conducted to determine the amount of oxygen that is available to the underlying tailings based on these results. The mass of oxygen entering the tailings if the cracks were allowed to exist for the full 12 months is shown in Figure 2.22. The contribution of each pressure gradient towards the mass flux can be determined based on the frequency of occurrence (Figure 2.18). The assumption was also made that a downward flux into the tailings exists for half the year, while during the other half of the year the upward flux would not contribute to the oxygen egress through the cracks as a result of barometric pumping.

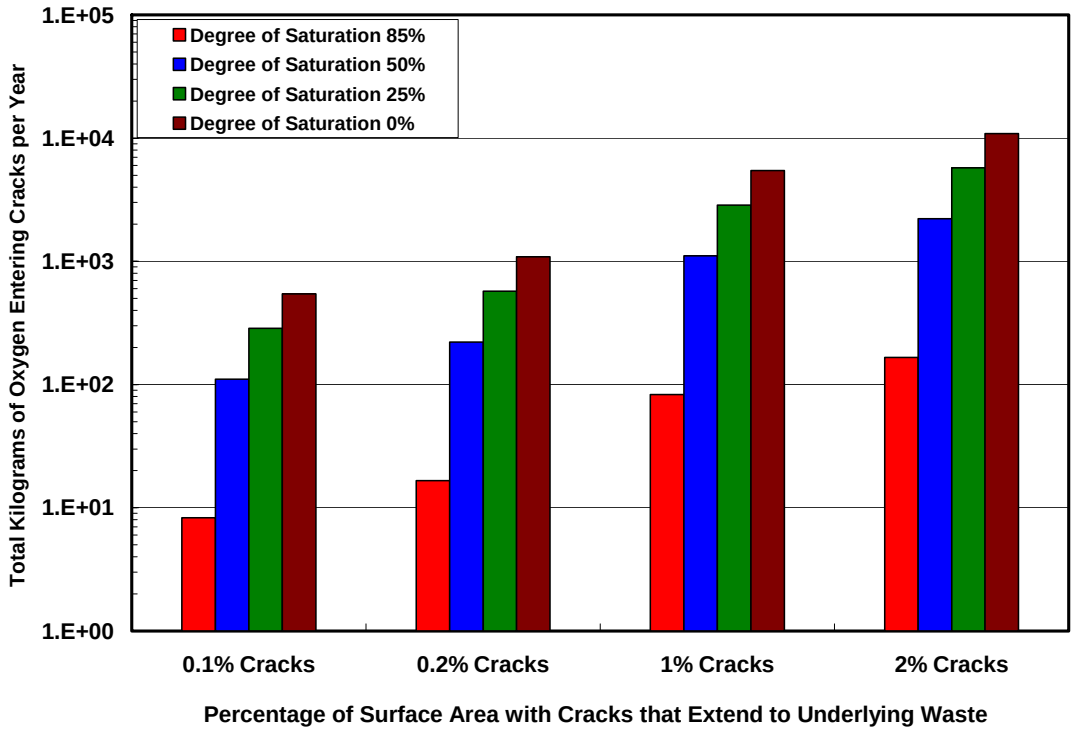

Figure 2.21 Mass of oxygen entering the underlying tailings material driven by barometric pumping based on crack percentage.

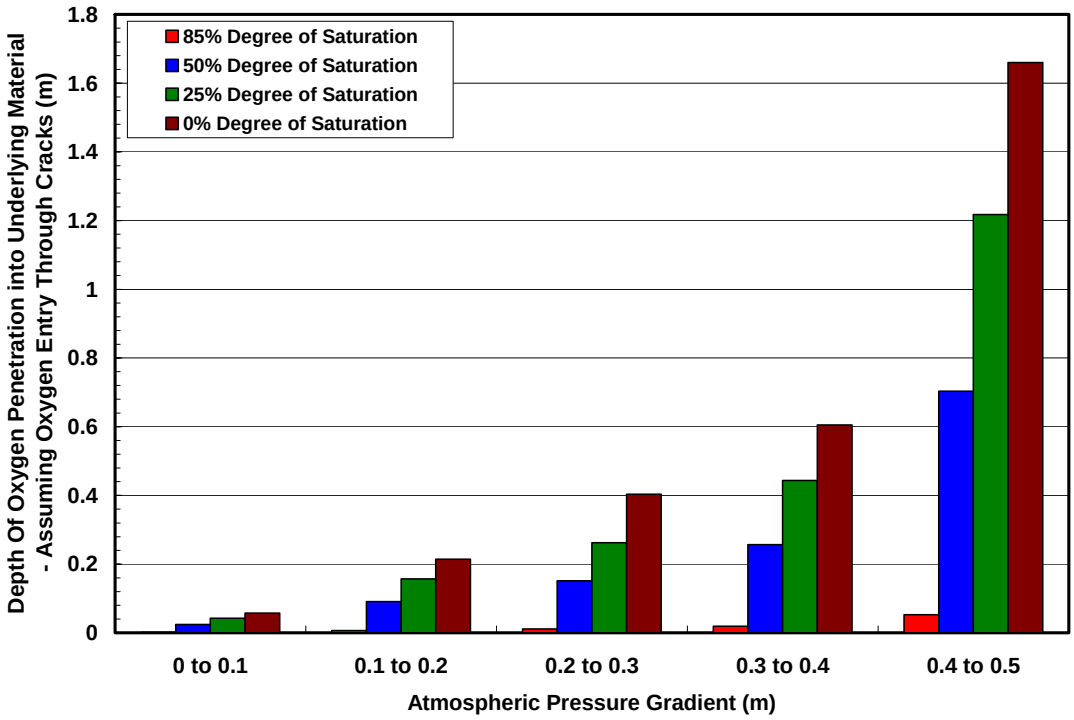

Figure 2.22 Penetration depth of atmospheric air into the underlying tailings material driven by barometric pumping.

2.4.1.3 Advection Through Water Filled Pores

Oxygen ingress will occur as a result of infiltration of oxygen-saturated water to the underlying waste material (advection). Infiltration rates of 50, 100, and 150 mm/yr, at oxygen-saturated water conditions, were evaluated for the example over a degree of saturation ranging from 0% to 100%, representing worst-case scenarios. Note that this is a conservative assumption because organic matter in the overlying soils will deplete some of the dissolved oxygen as it percolates down through the cover material. The calculated advective flux of oxygen is shown in Figure 2.23, assuming that water is oxygen-saturated at 10 mg/L. The advective oxygen flux is the greatest at saturation, due to the relationship between hydraulic conductivity and suction. The flux of oxygen due to advective forces at 50 mm/yr (saturated) is equal to the diffusion through pore-air space, or approximately 6×10^{-4} kg/year, as calculated by SoilCover (the SoilCover modelling is discussed in the following section).

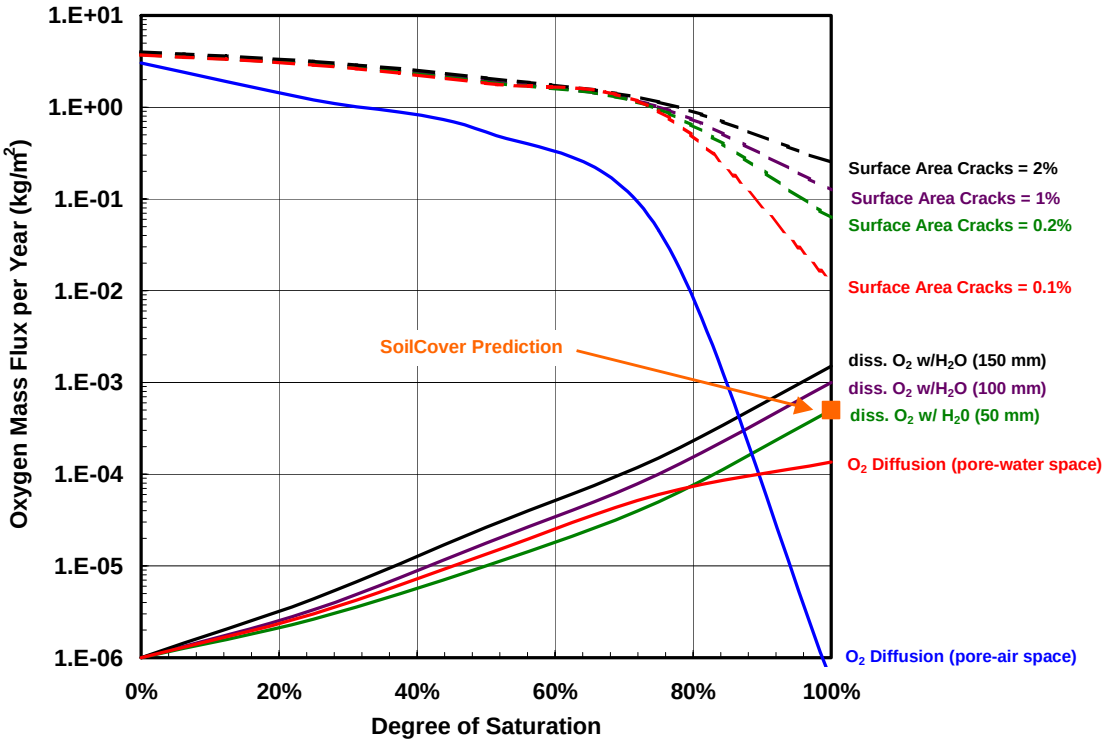

Figure 2.23 Mass flux of oxygen entering the tailings based on a 0.5 m cover barrier (0.5 m compacted layer assuming overlying growth medium does not impact on results, which is a conservative estimate). Diffusion through air and water, and advection through water is presented. Diffusion through pore-air space indicates the effects of surface cracking.

2.4.1.4 Diffusion Through Pore-Air and Pore-Water Space

The concept and theory behind diffusion of oxygen through pore-air and pore-water space was previously discussed in Section 1.4. Diffusion through the pore-air space of a cover system becomes significant at saturation levels below 85%. Typically a degree of saturation of 85% indicates the water content where the air phase becomes continuous within the porous media.

SoilCover, originally developed under MEND (MEND 1.25.1), can be used to predict oxygen diffusion through the pore-air space. SoilCover calculates the oxygen flux through porous media based on diffusion through the gas phase. The oxygen concentration gradient utilized to calculate the oxygen mass flux is based on the concentration at a user-defined node and the atmospheric oxygen concentration (i.e. 280 g/m^3).

The model simulation calculates a pressure head for each node of the modelled profile. The degree of saturation for each node is then obtained from a user-defined soil water characteristic curve, which in turn is used to calculate the effective coefficient of diffusion for oxygen (D_{eff}) at each node. The

user must specify either Millington and Shearer (1971) or Nicholson *et al.* (1989) to calculate D_{eff}. These relationships are based on a non-aggregated medium, which in general should restrict the application of these relationships to fine-textured cover layers such as typical compacted layers. Note that these relationships address oxygen diffusion through pore-air (i.e. SoilCover does not include oxygen diffusion through pore-water or advection of dissolved oxygen).

The SoilCover model was used to estimate the mass flux of oxygen through the pore-air space as shown in Figure 2.23.

In the previous section, the effects of cracks were evaluated with respect to barometric pumping, and in that scenario the oxygen flux included the crack surface only. Cracking of the cover surface that is not repaired could also lead to regions of de-saturation, increasing the oxygen diffusion rate into the underlying material. However, in this case the flux is based on the entire cover surface. The data presented in Figure 2.23 shows that the effect of an equivalent open area of 0.1% of the cover area which occurs as a result of cracking, will increase the oxygen diffusion rate by several orders of magnitude at 100% saturation. Caution is required when interpreting the effects of cracking on oxygen ingress shown in Figure 2.23, as the evaluation is on a yearly basis. In the unlikely event that lateral displacement cracks form (e.g. during a large magnitude earthquake), they should be identified and repaired promptly following the event.

REFERENCES

Aubertin, M., Bussière, B., Aachib, M., and Chapuis, R.P. 1996. Recouvrement multicouches avec effet de barrière capillaire pour contrôler le drainage minier acide : Étude en laboratoire et in situ. In Proceedings of the Symposium international sur les exemples majeurs et récents en géotechnique de l'environnement, Paris, ENPC-DCF, pp. 181-199.

Aubertin, M., Chapuis, R.P., Bouchentouf, A., and Bussière, B. 1997. Unsaturated flow modelling of inclined layers for the analysis of covers. In Proceedings of the Fourth International Conference on Acid Rock Drainage, Vancouver, BC, May 31-June 6, pp. 731-746.

Aubertin, M., Aachib, M., and Authier, K. 2000. Evaluation of diffusive flux through covers with a GCL. Geotextiles and Geomembranes. Vol. 18, pp. 215-233.

Barbour S.L., Wilson, G.W., and St-Arnaud, L.C., 1993. Evaluation of the saturated-unsaturated groundwater conditions at a thickened tailings deposit. Canadian Geotechnical Journal, Vol. 30, pp. 935-946.

Boldt-Leppin, B., O'Kane, M., and Haug, M.D. 1999. Soil covers for sloped surfaces of mine waste rock and tailings. *In* Proceedings of the Tailings and Mine Waste Conference, Fort Collins, Colorado, January 24-27, pp. 393-403.

Bouchet, R.J. 1963. Evapotranspiration reele at potentielle, signification climatique. Int. Assoc. Hydrol., Publication No. 62, pp. 134-142.

Bussière, B. and Aubertin, M., 1999. Clean tailings as cover material for preventing acid mine drainage: an in situ experiment. In Proceedings of Sudbury '99, Mining and the Environment II, Sudbury, Ontario, September 12-15, 1999, pp. 19-28.

Bussière, B., Aubertin, M., Morel-Seytoux, H.J., and Chapuis, R.P. 1998. A laboratory investigation of slope influence on the behavior of capillary barriers. *In* Proceedings of the 51st Canadian Geotechnical Conference, Edmonton, AB, October 4-7, pp. 831-836.

Bussière, B., Aubertin, M., and Chapuis, R.P. 2000. An investigation of slope effects on the efficiency of capillary barriers to control AMD. *In* Proceedings of the Fifth International Conference on Acid Rock Drainage, Denver, CO, May 21-24, pp. 969-977.

Bussière, B., Aubertin, M., and Julien, M. 2001. Couvertures avec effets de barrière capillaire pour limiter le drainage minier acide : aspects théoriques et pratiques. Vecteur environnement, 34: 37-50.

Bussière, B., Aubertin, M. and Chapuis, R.P. 2003. The behavior of inclined covers used as oxygen barriers. Canadian Geotechnical Journal. 40: 512-535.

CANMET. 2002. CANMET – CETEM Manual on Cover System Design for Reactive Mine Waste. June.

Chorley, R.J. 1978. The hillslope hydrological cycle. *In* Hillslope Hydrology. Edited by M.J. Kirkby. John Wiley & Sons Ltd., Chichester, pp. 1-42.

Fredlund, D.G. and Rahardjo, H. 1993. Soil Mechanics for Unsaturated Soils. John Wiley & Sons, Inc., New York, NY.

Fredlund, D.G., Barbour, S.L., and Pham H.Q. 2003. Evaluation of hysteresis models for predicting the boundary wetting curve. In Proceedings of the 2nd Asian Conference on Unsaturated Soils, UNSAT-ASIA 2003, April 15-17, Osaka, Japan, pp. 407-412.

Freeze, R.A. and Cherry, J.A. 1979. Groundwater. Prentice-Hall, Inc., Englewood Cliffs, NJ.

GeoAnalysis 2000 Ltd., 2001. SoilCover Version 5.2 User's Manual.

Glass, R.J. 1991. Laboratory research program to aid in developing and testing the validity of conceptual models for flow and transport through unsaturated porous media. SAND 89-2359, Sandia National Laboratory, Albuquerque, NM.

Gray, D.M. 1970. Handbook on the Principles of Hydrology. Canadian National Committee for the International Hydrological Decade.

Guymon, G.L. 1994. Unsaturated Zone Hydrology. Prentice-Hall Inc., Englewood Cliffs, NJ.

Hillel, D. 1980. Applications to Soil Physics. Academic Press, New York, NY.

Kisch, M. 1959. The theory of seepage from clay-blanketed reservoirs. Geotechnique. 9: 9-21.

Koliasev, F.H. 1941. Measures for the control of evaporation of soil moisture. Sbornik Rabot po Agronomi sheskoe Fiziki, Vol. 3, pp. 67-81.

Liakopoulos, A.C. 1965. Theoretical solution of the unsteady unsaturated flow problems in soils. Bulletin of the International Association of Science and Hydrology, 10: 5-39.

Maidment, D.R. 1993. Handbook of Hydrology. McGraw-Hill, Inc., New York, NY.

Mbonimpa, M., Aubertin, M., Aachib, M. and Bussière, B. 2003. Diffusion and consumption of oxygen in unsaturated cover materials. Canadian Geotechnical Journal. 40: 916-932.

MEND 1.25.1. 1996. SoilCover Users Manual Version 2.0. December.

MEND 2.22.2a. 1996. Évaluation en laboratoire de barrières sèches construites à partir de résidus miniers. March.

MEND 5.4.2d. 2001. MEND Manual: Volume 4 – Prevention and Control. February.

MEND 2.22.4b. 1999. Field performance of the Les Terrains Aurifères composite dry covers. April.

Millington, R.J. and Shearer, R.C. 1971. Diffusion in aggregated porous media. Soil Science, 111: 372-378.

Mitchell, J.K. 1976. Fundamentals of Soil Behavior. John Wiley & Sons, Inc. New York, NY.

Morel-Seytoux, H.J. 1992. The capillary barrier effect at the interface of two soil layers with some contrast in properties. HYDROWAR Report 92.4. Hydrology Days Publications.

Morris, C.E. and Stormont, J.C. (1997). Capillary barriers and Subtitle D covers: estimating equivalency. Journal of Environmental Engineering, 123: 3-10.

O'Kane, M. 1996. Instrumentation and monitoring of an engineered soil cover system for acid generating mine waste. M.Sc. Thesis, Department of Civil Engineering, University of Saskatchewan, Saskatoon, Saskatchewan, Canada.

O'Kane Consultants Inc. (OKC) 2000. Demonstration of the application of unsaturated zone hydrology for heap leach optimization. Report No. 628-1 prepared for IRAP, Contract #332407, September.

O'Kane, M., Barbour, S.L., and Haug, M.D. 1999. A framework for improving the ability to understand and predict the performance of heap leach piles. Paper presented at Copper '99, Phoenix, Arizona, October 10-13.

Penman, H.L. 1948. Natural evapotranspiration from open water, bare soil and grass. Proceedings of the Royal Society of London, Series A, Vol. 193, pp. 120-146.

Pham, H.Q., Fredlund, D.G., and Barbour, S.L. 2002. A simple soil-water hysteresis model for predicting the boundary wetting curve. In Proceedings of the 55th Canadian Geotechnical Conference, Niagara Falls, ON, October 20-23, pp. 1261-1267.

Pham, H.Q., Fredlund, D.G., and Barbour, S.L. 2003. Estimation of the hysteretic soil-water characteristic curves from the boundary drying curve. In Proceedings of the 56th Canadian Geotechnical Conference, Winnipeg, MB, September 29 – October 1. Vol 2: 115 – 121.

Pham, H.Q., Fredlund, D.G., and Barbour, S.L. 2003. A practical hysteresis model for the soil-water characteristic curve for soils with negligible volume change. Géotechnique. 53(2): 293-298.

Priestley, C.H.B. and Taylor, R.J. 1972. On the assessment of surface hear flux and evaporation using large-scale parameters. Monthly Weather Review, Vol. 100, pp. 81-92.

Rasmusson, A. and Erikson, J-C. 1986. Capillary barriers in covers for mine tailings dumps. Report 3307, The National Swedish Environmental Protection Board.

Richardson, C.W. and Ritchie, J.T. 1973. Soil water balance for small watersheds. Transactions of the ASAE, Soil and Water Division, pp. 72-77.

Ross, B. 1990. The diversion of capillary barriers. Water Resource Research, Vol. 26, pp. 2625-2629.

Scooter, D.R. 1978. Preferential solute movement through large soil voids. I. Some computations using simple theory. Australian Journal of Soil Research, Vol. 16, pp. 257-267.

Steenhuis, T.S., and Parlange, J.-Y. 1991. Comment on "The diversion capacity of capillary barriers" by Benjamin Ross. Water Resources Research. 27(8): 2155-2156.

Stephens, D.B. 1996. Vadose Zone Hydrology. Lewis Publishers, New York, 347 pp.

Stormont, J.C. 1995. The effect of constant anisotropy on capillary barriers. Water Resource Research, Vol. 31, pp. 783-785.

Stormont, J.C. 1996. The effectiveness of two capillary barrier on a 10% slope. Geotechnical and Geological Engineering, Vol. 14, pp. 243-267.

Swanson, D.A. 1995. Predictive modelling of moisture movement in engineered soil covers for acid generating mine waste. M.Sc. Thesis, University of Saskatchewan, Saskatoon, Saskatchewan, Canada.

Swanson, D.A. and O'Kane, M. 1999. Application of unsaturated zone hydrology at waste rock facilities: design of soil covers and prediction of seepage. *In* Proceedings, 16th Annual National Conference, American Society for Surface Mining and Reclamation, Scottsdale, Arizona, August 13-19, pp. 517-526.

Thornthwaite, C.W. 1948. An approach toward a rational classification of climate. Geological Review, Vol. 38, pp. 55-94.

Vanapalli, S. 1994. Simple test procedures and their interpretation in evaluating shear strength of an unsaturated soil. Ph.D. Thesis, University of Saskatchewan, Saskatoon, Saskatchewan, Canada.

Whipkey, R.Z., and Kirkby, M.J. 1978. Flow within the soil. *In* Hillslope Hydrology. Edited by M.J. Kirkby. John Wiley & Sons Ltd., Chichester, pp. 177-225.

Wilson, G.W. 1990. Soil evaporative fluxes for geotechnical engineering problems. Ph.D. Thesis, University of Saskatchewan, Saskatoon, Saskatchewan, Canada.

Wilson, G.W., Fredlund, D.G. and Barbour, S.L. 1994. Coupled soil-atmosphere modelling for soil evaporation. Canadian Geotechnical Journal. Vol. 31, pp. 151-161.